



DEGREE PROJECT IN VEHICLE ENGINEERING,  
SECOND CYCLE, 30 CREDITS  
*STOCKHOLM, SWEDEN 2019*

# **Steering system development using test rig and driving simulators**

**UTSAV KHAN**

**ANDREA BIANCHI**

**KTH ROYAL INSTITUTE OF TECHNOLOGY  
SCHOOL OF ENGINEERING SCIENCES**

---

## Abstract

Conventional model-based development approaches such as Model-in-Loop (MiL) and Software-in-Loop (SiL) have been used in electric power assisted steering (EPAS) development in recent years, but when it involves a physical motor and the vehicle communication network, the development mostly comes down to real vehicle testing and tuning. The objective and outcome of this master thesis is to develop a Hardware-in-Loop (HiL) environment that involves the real EPAS powerpack and human Driver-in-Loop (DiL) using a static driving simulator. The focus is on the study of the performance of the HiL rig in terms of its ability to reproduce steering related Objective Metrics (OMs).

In this thesis work, the initial part deals with the study of EPAS systems, HiL test-rigs, objective metrics and real-time simulation environment. The second part deals with the modeling and verification methods of an EPAS system along with HiL test-rigs using high and low fidelity vehicle models and steering systems in the MiL and SiL environment.

As this thesis work deals with the HiL test rig, some practical problems were faced. These involve implementation and HiL architecture, data transmission between the test rig and the real time simulation environment with rest-bus simulation. Several HiL test-rig issues and limitations are addressed: 1. EPAS torque measurement noise; 2. System bandwidth limitation from control and hardware perspectives; 3. Simulation model; 4. System delays and cogging.

Due to these drawbacks the testing scenarios are currently limited between low to mid-frequency vehicle manoeuvres. OM values from HiL simulations accurately compare with real-test data, but the subjective steering feel can still be quite different which is not represented by OM<sub>s</sub>. Furthermore, the system can be improved by smoothing the reference and control signals by an implementation of low-pass filters or observers, and potentially by different servo control strategies and compensators. Once fully functional, the HiL simulation will be useful during early stage steering system development, being sensitive to changes in a similar way to a real vehicle during testing.

## Sammanfattning

Konventionella modellbaserade utvecklingsmetoder såsom Model-in-Loop (MiL) och Software-in-Loop (SiL) har använts inom utvecklingen av elektriskt servoassisterad styrning (Electric Power Assisted Steering, EPAS) under de senaste åren, men när det handlar om en fysisk motor och kommunikation huvudsakligen med fordonets nätverk, så sker utvecklingen oftast med verkliga fordonstest med nödvändig justering. Syftet och målet med detta examensarbete är att utveckla en HiL-rigg (Hardware-in-Loop) som involverar det verkliga EPAS systemet och Driver-in-Loop (DiL) med hjälp av en statisk körsimulator, där fokus ligger på att studera prestandan för HiL-rigg och dess förmåga att återskapa styrrelaterade Objektiva Mätetal (OM).

I detta examensarbete består den inledande delen av studien av EPAS-system, HiL-test-riggar, Objektiva mätetal samt realtidssimuleringsmiljö. Den andra delen består av modellerings- och verifieringsmetoder för ett EPAS-system tillsammans med HiL-testriggar med fordonsmodeller med hög och låg trovärdighet och styrsystem i MiL- och SiL miljöer.

Då detta examensarbete involverar en HiL-testrigg har vissa praktiska problem uppstått. Bland problemen var implementering och HiL-arkitektur, dataöverföring mellan testriggen och realtidssimulering med rest-bus simulering. Flertalet problem med en HiL-testrigg och dess begränsningar har behandlats: 1. EPAS-brus i vridmomentmätning; 2. Systembandbredds begränsning från regler- och hårdvaroperspektiv; 3. Simuleringsmodell; 4. Systemfördröjningar och ojämnt vridmoment från elmotorn.

På grund av dessa nackdelar är testscenarierna för närvärande begränsade till fordonsmanövrar med låga till mellanfrekvensområden. OM-värden från HiL-simuleringar stämmer överens med verkliga testdata, men den subjektiva styrkänslan kan fortfarande känna ganska annorlunda vilket inte är representerat av OMs. Dessutom kan systemet förbättras genom att referens- och styrsignaler filtreras genom implementering av lågpassfilter eller observatörer, samt med olika servoreglertekniker och kompensatorer. När systemet är fullt funktionellt kan HiL simuleringen vara användbar vid utvecklingen av styrsystemet i ett tidigt skede, då det är känsligt för förändringar likt ett verkligt fordon under testning.

## Acknowledgements

We would like to take this opportunity to express our sincere gratitude and appreciation to our Industrial supervisor Weitao Chen and Matthijs Klomp for sharing the knowledge and your valuable time. The weekly reviews and meetings, the continuous support proved really valuable. We are really thankful to Carl Sandberg for welcoming us to the Vehicle Dynamics CAE team and giving us the opportunity to work with a great team in a motivating environment.

We would also like to thank Max Boerboom, Dr. Shenhai Ran, Marcus Ljungberg, Riccardo Zoccarato and Mohit Asher for their extended support. We really appreciate your effort to take time out from your busy schedule to discuss issues and suggest solutions whenever we requested. A special thanks goes to our academic supervisor Lars Drugge for assisting us throughout the Master Thesis with guidance and suggestions to develop the thesis. Feedback and suggestions from Lars was really crucial for completion of this project.

Many thanks to Eshwar Sondhi, Alejandro Gonzalez and Simon Schoutissen for helping us with the simulation models and cooperating in-terms of scheduling of work on the HiL. Our heartfelt thanks to Mattias Savinainen for supporting us throughout the project with CAN simulation. We would also like to thank VecScan AB for providing us with very important licenses and training session which turned out to be very crucial throughout the project.

We would also like to not forget about the great friendship and support from our classmates as well as co-workers, Ankur, Ansh and Chitranjan for hundreds of discussion over lunch time, sharing experience throughout this project and balancing our Master Thesis time with fun-filled weekend times. Finally we would like to thank our families for the continuous support and keeping faith on us.

Regards,  
Utsav and Andrea  
Gothenburg, 2019

# Contents

<b>Abstract</b>	i
<b>Sammanfattning</b>	ii
<b>Acknowledgements</b>	iii
<b>List of Figures</b>	vii
<b>1 Introduction</b>	1
<b>2 Background</b>	2
2.1 Electric Power Assisted Steering . . . . .	2
2.2 Hardware-in-Loop . . . . .	3
2.3 HiL servo motor . . . . .	4
2.4 IPG Carmaker . . . . .	4
2.5 Objective metrics and test scenarios . . . . .	5
<b>3 Vehicle and Steering models</b>	12
3.1 Steering model . . . . .	12
3.2 Vehicle model . . . . .	14
3.3 Steering behaviour study . . . . .	15
<b>4 Verification Method</b>	18
4.1 Model in Loop . . . . .	18
4.1.1 Model description . . . . .	18
4.1.2 Performance analysis . . . . .	19
4.2 Software in Loop . . . . .	21
4.2.1 PSCM Software-in-Loop model . . . . .	21
4.2.2 IPG Carmaker implementation . . . . .	21
4.2.3 Pfeffer steering model . . . . .	22
4.2.4 PSCM SiL model integration . . . . .	23
4.2.5 PID based driver model . . . . .	23
4.2.6 Delay modeling . . . . .	24
<b>5 Powerpack HiL test rig</b>	25
5.1 Literature review . . . . .	25
5.2 HiL architecture . . . . .	26
5.2.1 Hardware . . . . .	28
5.2.2 Software . . . . .	28
5.2.3 Communication . . . . .	28
5.3 System identification . . . . .	28
5.4 Steering test rig control . . . . .	32
5.5 Autonomous driving mode test capability . . . . .	33
<b>6 Static driving simulator</b>	35
6.1 Overview . . . . .	35
6.2 Architecture . . . . .	35

<b>7 Results</b>	<b>38</b>
7.1 Comparison of Objective Metrics . . . . .	38
7.1.1 On-center . . . . .	38
7.1.2 Low-G swept steer . . . . .	41
7.1.3 High-G swept steer . . . . .	42
7.2 Effect of parameter variation on Subjective Assessment . . . . .	43
<b>8 Test rig control and limitations</b>	<b>45</b>
8.1 Hardware limitations . . . . .	45
8.1.1 Added inertia . . . . .	45
8.1.2 Torque ripple . . . . .	45
8.1.3 Transmission delays . . . . .	46
8.1.4 Measurement errors . . . . .	47
8.2 Software limitations . . . . .	47
8.2.1 Servo motor control strategy . . . . .	47
8.2.2 Vehicle and steering models . . . . .	48
8.2.3 Driver model . . . . .	48
<b>9 Conclusions and Future work</b>	<b>49</b>
<b>References</b>	<b>52</b>

## List of Figures

1	HPS vs EPAS Systems Complexity [1] . . . . .	2
2	EPAS Types and Performance [1] . . . . .	3
3	Three primary components of an HiL: Operator interface, Real-time PC with I/O module and ECU with hardware to be tested . . . . .	4
4	IPG Carmaker Virtual Vehicle Environment Representation . . . . .	5
5	Steering wheel input for Parking Effort . . . . .	6
6	Steering wheel input for On-Center . . . . .	7
7	Steering wheel input for frequency response . . . . .	7
8	Steering wheel input for Swept steer . . . . .	8
9	EPAS system with axle-parallel drive . . . . .	12
10	Bicycle model . . . . .	14
11	Frequency Response Analysis of Vehicle and Steering models. 1. The EPAS is not included in the model (blue). 2. The EPAS, belt and ballnut gear are modeled, but no assist is given (orange). 3. The EPAS is operational, but only uses its basic boost curves function (yellow). 4. The complete EPAS ECU is modeled, meaning the motor also uses functions such as inertia compensation, damping, steering return etc (purple). . . . .	16
12	Characteristics of MiL, SiL and HiL . . . . .	18
13	MiL Block Diagram . . . . .	19
14	Inertia Effect on Load Motor - Stiff PID . . . . .	20
15	Inertia Effect on Load Motor - Untuned PID . . . . .	20
16	PSCM SiL model . . . . .	21
17	"Car and Trailer" subsystem of the Simulink Model in Carmaker . . . . .	22
18	Mechanical module of the steering model with forces and direction of motion	23
19	Driver model . . . . .	24
20	Pade approximation comparison for a step response . . . . .	24
21	Example of conventional steering testrig . . . . .	25
22	Example of powerpack steering testrig . . . . .	26
23	Actual image of the Powerpack HiL along with Brake HiL at VCC . . . . .	26
24	HiL architecture . . . . .	27
25	ISO view of the powerpack HiL . . . . .	27
26	Generalized Load Motor Torque Control . . . . .	29
27	Generalized Load Motor Velocity Control . . . . .	29
28	Generalized Load Motor Position Control . . . . .	30
29	IPG Carmaker Maneuver GUI . . . . .	30
30	Bode plot of load motor system identification . . . . .	31
31	Coherence plot of load motor system identification . . . . .	32
32	Bode plot from static simulator servo motor system identification . . . . .	32
33	Steering system and powerpack testrig correlation . . . . .	33
34	Static driving simulator at Volvo Cars Corporation . . . . .	36
35	Static driving simulator at Volvo Cars Corporation - Steering Column . . . . .	36
36	Driving simulator architecture with HiL . . . . .	37
37	SDNA OMs for On-Centre maneuver . . . . .	38
38	ay vs SWT for On-center . . . . .	39
39	ay vs SWA for On-center . . . . .	39
40	yawrate vs SWA for On-center . . . . .	40

41	SWA vs SWT for On-center . . . . .	40
42	Effect of different low-pass filter cutoff frequency for kistler sensor measurement . . . . .	41
43	SDNA OM <sub>s</sub> for LSS maneuver . . . . .	42
44	SDNA OM <sub>s</sub> for HSS maneuvers . . . . .	42
45	Effect of vehicle parameter changes on steering behaviour where (a) Effect of change of tires (b) Effect of change of pinion to rack ratio (c)Effect of increase in EPAS assist . . . . .	44
46	Suggested Hardware Change for Inertia Compensation . . . . .	45
47	Servo Motor Torque Ripple . . . . .	46
48	Lead Compensator Example . . . . .	47

## Abbreviations

- ADAS** Advanced Driver Assistance System
- COG** Center of gravity
- DiL** Driver-in-Loop
- ECU** Electronic Control Unit
- EPAS** Electric Power Assisted Steering
- EPSapa** Electric Power Steering Axial Parallel
- EPSc** Electronic Power Steering Column
- EPSdp** Electric Power Steering Dual Pinion
- EPSp** Electric Power steering pinion
- FR** Frequency Response
- HiL** Hardware-in-Loop
- HPS** Hydraulic Power System
- HSS** High-g Swept Steer
- LM** Load/Servo motor
- LSS** Low-g Swept Steer
- MiL** Model-in-Loop
- OC** On-center
- PE** Parking Effort
- PSCM** Power Steering Control Module
- SiL** Software-in-Loop
- SWA** Steering Wheel Angle
- SWT** Steering Wheel Torque
- VCC** Volvo Car Corporation

# 1 Introduction

In the automotive industry, both physical testing and CAE simulations play a fundamental role in vehicle development. In an engineering environment, two important types of simulations are software-based and combined software/hardware simulations, also known as HiL simulations. Using a HiL setup allows to increase the accuracy of the simulation results by replacing parts of the analytical models with real hardware. Using this approach, the actual hardware non-linearities and limitations are implemented in the simulation without the need of modeling them. HiL simulations may provide several advantages over real tests, such as decreased cost and development time, while providing a relatively high degree of accuracy.

A HiL setup can be any combination of software and hardware. In this research, the focus is on the study of a EPAS powerpack HiL rig used by Volvo Cars. It was originally used for different motion control algorithm testing and development but the idea of using the same test rig for steering system development by the Vehicle Dynamics CAE team was born at Volvo and was the basis of this thesis work. In this test rig, the vehicle and steering models run on a real-time machine, while the EPAS motor is operated in closed-loop with the analytical models, using a direct coupling to a servo motor.

The aim of this project is to identify and quantify the limitations (delays, noise, tuning of control strategies) of the servo motor and complete HiL rig, which arise from the nature of the hardware and software being used. The impact of these limitations on the simulation results, such as OM values, gives an indication of the range of operation in which the HiL rig can provide reliable results. Another goal of the project is to provide useful suggestions on how to modify the setup, both from a software and hardware perspective, in order to improve its range of operation. The research question of this thesis project can therefore be formulated as:

***What are the servo motor and complete HiL rig limitations and to what degree do they hinder the rig range of application? What can be improved in the future to achieve improved performance?***

The report is structured in the following way. In section 2, the knowledge gathered from the thesis literature study performed during this master thesis is presented; in section 3, a study of the EPAS system, vehicle and steering models behaviour was conducted; in section 4, the HiL simulation environment was replicated in MiL and SiL for learning and verification purposes; in section 5, a more in-depth study of the steering HiL rig is performed and its operation is explained; in section 6, the DiL is introduced into the simulation environment; in section 7, a comparison between SiL, HiL and real-test data and OMs is performed, also subjective feedback from the DiL simulation is discussed; in section 8, the HiL rig limitations are discussed and suggestions on how to improve the HiL rig performance are given; in section 9, conclusions are drawn and future work for improvement of the HiL rig performance is suggested.

## 2 Background

### 2.1 Electric Power Assisted Steering

Original steering systems used to be fully operated by the driver, with no assist torque being provided by additional components. Even if this concept is still being used in specific cases, the vast majority of passenger vehicles slowly switched to power assisted steering systems. The first, and most common until a few years ago, is the Hydraulic Power Steering (HPS), which introduces a steering aid through a hydraulic mechanism including a series of valves and pumps. This system has several downsides, such as the continuous power consumption due to the constant operation of the pumps (even during engine idle), high complexity and low packaging efficiency due to the large number of components (Figure 1), missing active driver assist (ADAS) capabilities. The EPAS resolves to a high extent all the issues which comes with a HPS system. In fact, an EPAS only operates when steering torque is applied by the driver, it has fewer components and can be used for driver assistance or autonomous purposes [1] as well.

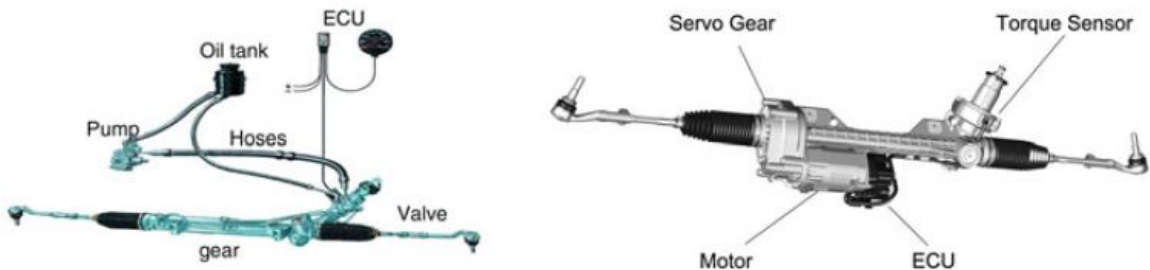


Figure 1: HPS vs EPAS Systems Complexity [1]

EPAS systems only involve a limited amount of components, as shown in Figure 1. Regardless of the specific EPAS type, these systems all have an electric motor, used to provide the assist torque, ECUs to control the electric motor and communicate to the rest of the nodes on the CAN bus, gearing to amplify the motor torque, and a torque sensor located on the torsion bar, which measures the torsion bar torque and feeds it to the EPAS ECU as an input.

There are several different types of EPAS systems being used on passenger vehicles. The most common ones are EPSc, EPSdp and EPSapa. All configurations have an EPAS motor, ECUs, gearing for torque amplification and a torque sensor in common. However, there are several differences. EPSc is a system where the EPAS motor is located on the steering column. It is mainly used for low assist torque requirements. In EPSp and EPSdp, the electric motor is placed at the steering pinion or at an additional pinion added on the rack. These are mainly used for medium assist torque requirements. EPSapa has the electric motor placed parallel to the rack and it is connected to it using a belt and ball-nut gear, which amplify the torque to a relatively large extent. The EPSapa is suitable for high assist torque requirements [2] [1]. Figure 2 displays the performance and torque operation range of the different EPAS systems.

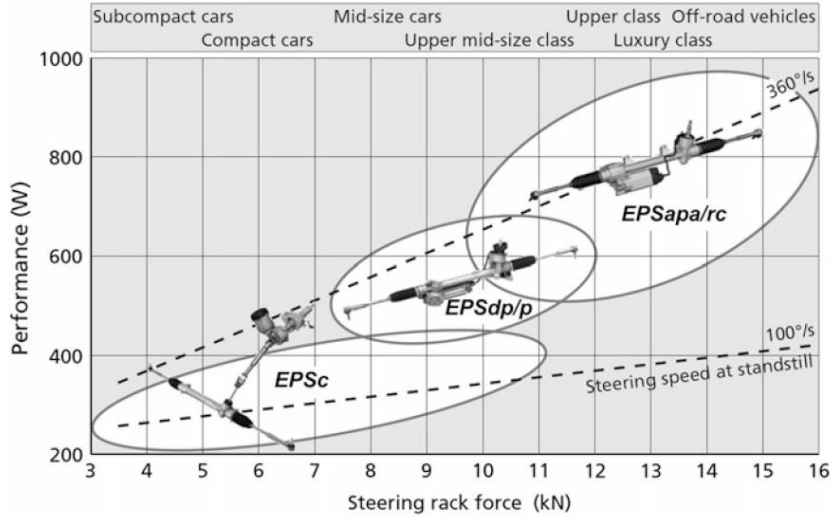


Figure 2: EPAS Types and Performance [1]

It was fundamental to have an adequate background knowledge on the operation of a EPAS system for this thesis because it is one of the main components used in the steering hardware-in-loop test rig used at Volvo Cars for steering development and testing.

## 2.2 Hardware-in-Loop

In this project, a steering Hardware-in-Loop (HiL) system is studied and techniques to improve its performance are implemented.

Hardware-in-Loop is a technique used to test and validate designs of complex embedded systems where real signals coming from a sensor, actuator or controller are connected to a simulation environment, tricking the component to think that it is working in the real finished product. Different test scenarios can be performed in a cost and time efficient way. Quality and reliability of HiL test results lie between the reliability of pure model-based simulation and real vehicle testing. HiL testing always includes the emulation of electrical components, which act as an interface between the simulation of the plant model and the system under testing [3] [4].

In this thesis work, the EPAS is the hardware present in the HiL, the vehicle is simulated using a real-time machine and the interface between the virtual model and hardware is made up of a servo motor, also called Load Motor (LM) in this thesis work, and communication cables which use different protocols. Figure 3 represents the primary components of an HiL system and method of communication between them.

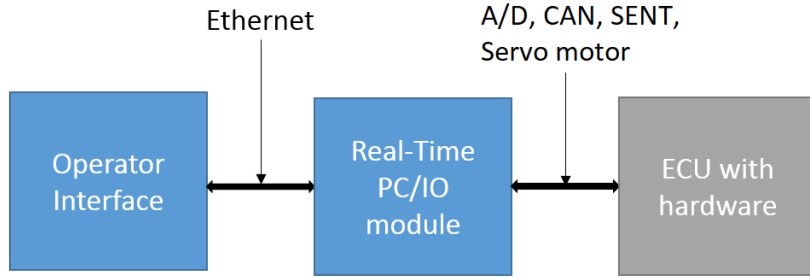


Figure 3: Three primary components of an HiL: Operator interface, Real-time PC with I/O module and ECU with hardware to be tested

### 2.3 HiL servo motor

Servo motors were introduced during the 20th century in order to allow motion control in production processes. This permitted to have increasing levels of automation which improved production efficiency [5]. A servo motor is an electric motor whose purpose is to accurately follow requests sent by an user. There are three types of requests which can be sent to a servo motor: position, velocity and torque. Once a request is sent as a signal, it first passes through a servo drive. The servo drive is an electronic unit which works as a signal amplifier and contains the control strategy for the servo motor. The servo drive control strategy is made up of a series of nested feedback loops: torque is the innermost loop, position is the outermost loop and velocity is in between the two. These are inserted with the goal of increasing the system's accuracy when reacting to a request, and also for different control purposes [5]. Thus, the servo drive receives a target value of a specific variable of choice (position, velocity or torque) from the user, which is compared to the actual parameter value that the servo motor is delivering: the error between the two is then reduced by the control strategy of the servo drive.

The servo motor is a crucial subsystem of the HiL steering rig which was studied throughout this project. It is used to simulate the rack motion at the EPAS motor end (thus, rack motion converted to rotational motion after appropriate ratios). The servo motor was a main focus of the investigation considering the performance of the HiL rig since it acts as the main interface between the real-time virtual vehicle simulation (performed in IPG Carmaker) and real hardware simulation (EPAS motor).

### 2.4 IPG Carmaker

IPG Carmaker is a virtual testing application for automobiles. The three main elements of a Carmaker simulation are the vehicle, driver and road, which, when used together, make up the so called Virtual Vehicle Environment [6].

## The Virtual Vehicle Environment

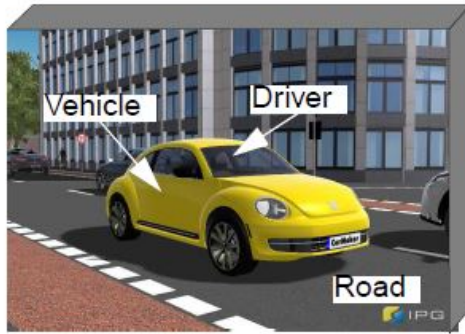


Figure 4: IPG Carmaker Virtual Vehicle Environment Representation

In this thesis work, Carmaker HiL is used due to the presence of real hardware in the loop. However, the Virtual Vehicle Environment can be altered according to the simulation setup. Several real hardware systems can be introduced in the setup and the corresponding mathematical models within Carmaker can be disabled/changed. For example, a real EPAS, PSCM and in certain cases even a real driver are used in this project, which can replace the equivalent Carmaker mathematical models.

## 2.5 Objective metrics and test scenarios

According to the research question, an important objective of the thesis was to identify which test maneuvers and Objective Metrics (OMs) can be tested on the powerpack HiL rig with relative accuracy and which are comparatively poor in test results. Volvo Cars uses close to 30 predefined objective metrics to define its steering DNA and each of the OMs are associated with different testing maneuvers. The major Steering DNA (SDNA) tests are Parking Effort (PE), On-center (OC), Frequency Response (FR), Low-g Swept Steer (LSS) and High-g Swept Steer HSS.

### Parking Effort

The purpose of this test is used to characterize the steering torque the driver needs to apply during slow speed parking and during parking in stand still condition.

For the static parking maneuver, while the vehicle is completely stand still, turn the steering wheel to lock in one direction and then lock in the other direction. This should be continued until the steering wheel is back to straight ahead position i.e. after 1.5 cycles. The preferred steering wheel wave form is triangular.

For the rolling parking maneuver, the vehicle should be moving at a very low (approx 7 km/h) constant speed in a straight line, then repeat the same maneuver as the static parking test. Figure 5 shows the steering angle input with respect to time for parking effort maneuver.

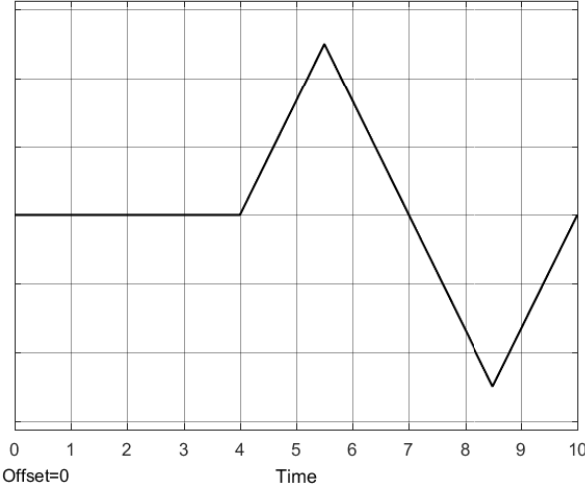


Figure 5: Steering wheel input for Parking Effort

## On-center

On-center steering test is used to characterize vehicle handling at low steering frequency and low lateral acceleration. Also, as stated by Norman [7], road feel at low accelerations or small steering angles similar to the on center events are of interest and is intended to measure performance in a range typical of highway driving and on roads requiring mild to moderate turning.

The test is conducted at different speeds and different lateral acceleration levels. Low acceleration turning events characterize steering performance during corrections while driving on a straight road and moderate lateral acceleration turning events characterize performance on a road with multiple left and right hand turns.

While performing this test, the vehicle is driven on a straight path at velocities ranging from 20-150 km/h (constant velocity kept for each test) during different test runs and a sine wave steering wheel input at 0.2 Hz frequency is given. The magnitude of the steering wheel angle depends on desired peak lateral acceleration (from low to moderate) at a given speed. The steering wheel angle corresponding to peak lateral acceleration is identified using pre-events such as ramp steer. While performing on-centre tests, quantities such as SWA, SWT, yaw rate, lateral acceleration and vehicle longitudinal velocity are logged, which are then used for cross plots corresponding to different OMs. Figure 6 shows the steering angle input over time for on-center maneuver.

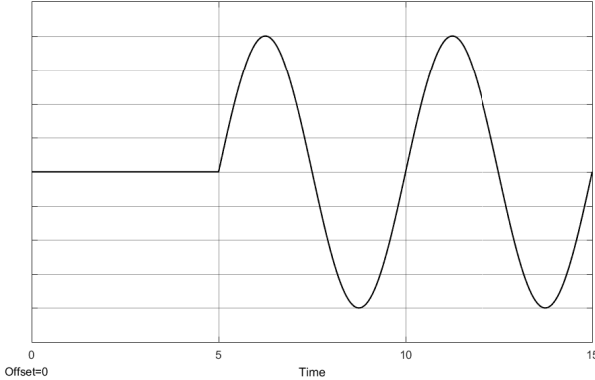


Figure 6: Steering wheel input for On-Center

## Frequency Response

Frequency response is one of the open-loop test methods used to assess the steady-state and transient handling performance of a vehicle in the linear driving range i.e. all the maneuvers where lateral acceleration levels are between low and moderate. Frequency response tests performed at Volvo Cars quite closely follow the SS-ISO 7401:2011 standard.

The test is conducted at two different velocities 75 km/h and 120 km/h and initially the vehicle is driven on a straight path maintaining constant speed. A sine wave SWA input is given, which results in a moderate lateral acceleration at a frequency of less than 0.2 Hz. The frequency range of this input wave is varied from 0.2 Hz to 3 Hz and ideally the input starts with higher frequency and is ramped down to low frequency. The reason behind doing high to low frequency is to limit the usage of road by the vehicle while performing the maneuver. Throughout this maneuver, SWA, SWT, yaw velocity, lateral acceleration, roll angle, side-slip angle (optional) and vehicle longitudinal velocity are measured. Figure 7 shows the steering angle input over time for frequency response maneuver.

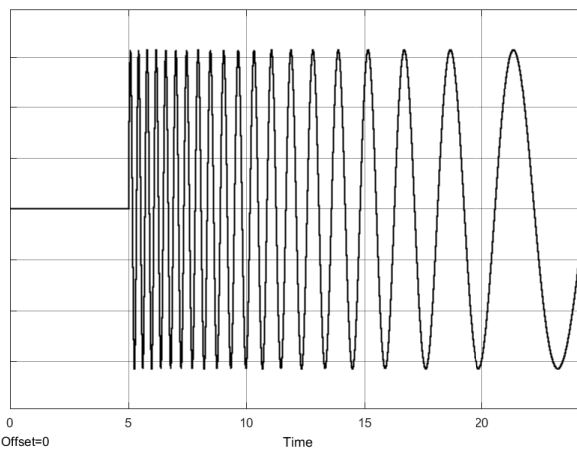


Figure 7: Steering wheel input for frequency response

## Low-g and High-g Swept Steer

The reason of performing a low-g swept steer is to analyze steering performance in minor steering events and correction maneuvers while driving straight on a highway. High-g swept steer is used to analyze the steady-state cornering of a vehicle. Steady-state directional and roll dynamics from normal cornering condition to handling limits can be tested in this maneuver.

In both high and low-g swept steer the vehicle is driven in a straight line at a speed of 75 km/h and then the steering wheel angle is increased slowly until 0.15 g lateral acceleration is achieved for low-g swept steer, while maximum lateral acceleration of the vehicle is achieved for high-g swept steer. Parameters measured during this test are same as of FR. Figure 8 shows the steering angle input over time for swept steer maneuver.

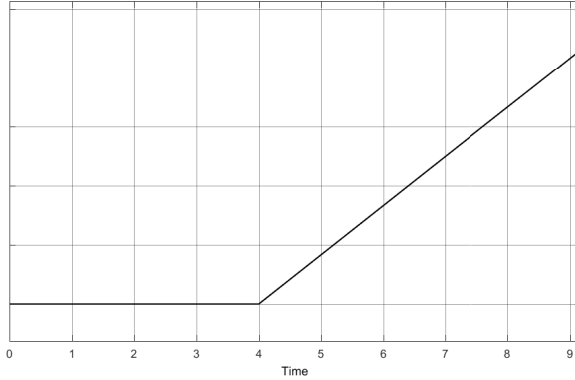


Figure 8: Steering wheel input for Swept steer

A selected number of OMs were chosen to be tested on the powerpack rig as seen in Table 1. OMs are divided into three major subgroups according to steering attributes.

Table 1: Objective Metrics and test maneuver

Test Cases	Measured Variables	Derived Metrics	Condition
On-Center	SWA	Response gain straight path	0.2g 120km/h
	SWT	Lateral acceleration response gain	0.2g 80km/h
	Yaw Rate	Lateral acceleration response gain	0.2g 120km/h
	Lat. Acceleration	Friction feel	0.2g 120km/h
	Vehicle Velocity	Yaw response gain	0.4g 80km/h
		Response gain linearity	0.4g 80km/h
Low-g Swept Steer	SWA	On-center hysteresis	0.4g 80km/h
	SWT	Off-center hysteresis	0.4g 80km/h
	Lat. Acceleration	Window	120km/h
	Vehicle Velocity	Gain Linearity	120km/h
	Roll Angle	Torque Deadband	120km/h
	SWA	Torque Buildup	120km/h
High-g Swept Steer	Front Wheel Angle	On-center torque gradient	75km/h
	SWT	Response Gain Understeer	75km/h
	Yaw Rate	Roll Control Cornering	75km/h
	Lat. Acceleration	Torque Buildup Cornering	75km/h
	Vehicle Velocity	Effort Level	75km/h
	Roll Angle		
Parking Effort	SWA	Sideslip Angle	
	SWT		
Parking Effort	Vehicle Velocity	Parking Efforts Standstill	0km/h
		Parking Efforts Rolling	7km/h

## Straight Ahead Controllability

### Window

Defines the amount the steering wheel can be turned before the car actually starts turning.

### Response Gain Straight Path

Defines the change of vehicle yaw rate as the steering wheel is moved in the on-center range.

### Lateral Acceleration Response Gain

Defines the change of vehicle lateral acceleration as the steering wheel is moved in the on-center range.

### Gain Linearity

Defines the linearity of the lateral acceleration relative to the SWA i.e. slope of the SWA vs lateral acceleration plot.

### Torque Deadband

It can be interpreted as a steering play i.e. a smaller deadband means that the SWT rises rapidly from a straight ahead position and the steering feel is connected.

### Torque Build-up

Defined as the average SWT/g slope at a torque of 1.3 Nm until when 0.1 g lateral acceleration is reached.

### Friction Feel

The torque needed to initially turn the steering wheel. It is normally defined as half of the hysteresis torque at 0 g lateral acceleration for an on-center maneuver.

## Cornering Controllability

### Yaw Response Gain

It is the same as the response gain straight path metric but at a higher lateral acceleration.

### Response Gain Understeer

Describes the amount of increase in SWA needed with increasing lateral acceleration for a constant radius corner, i.e. same as the understeer gradient.

### Response Gain Linearity

Defines the linearity of the yaw rate relative to the SWA i.e. slope of the SWA vs yaw rate plot.

### Roll Control Cornering

Defined as the total steady-state roll (roll of vehicle body relative to ground) expressed as deg/g.

### On-center Torque Gradient

Defined as torque gradient in the on-center region expressed as Nm/g.

**Torque buildup cornering**

Defined as torque gradient outside the on-center region expressed as Nm/g.

**On-center Hysteresis**

Defined as the hysteresis in degrees as the steering wheel torque passes zero when turned from left and right direction during on-center.

**Off-center Hysteresis**

It is a similar measurement as friction feel, but measured at a higher lateral acceleration. This metric defines the effort needed to make a small steering correction while taking a turn.

**Effort Level**

Defined as the steering torque needed at 0.3 g lateral acceleration i.e. effort required to turn the steering wheel at a higher lateral acceleration.

**First Impression****Parking Efforts Standstill**

Defined as the SWT required for turning the steering wheel from 180 degrees left to 180 degrees right while standstill.

**Parking Efforts Rolling**

Defined as the SWT required for turning the steering wheel from 180 degrees left to 180 degrees right while moving at a very slow speed.

### 3 Vehicle and Steering models

In this section, analytical models of a basic vehicle and steering systems were developed. Moreover, a study on the dynamic behaviour of the models was conducted. The goal was to gain knowledge on the workings of a steering with EPAS system and understanding the effect of an EPAS system on the steering and vehicle systems.

#### 3.1 Steering model

In order to understand the EPAS system, it was very important to model the force equations. In this thesis, the EPSapa was used since most of the vehicles at Volvo Cars used it. EPSapa is different from the EPSdp as the torque assistance is being transferred to the rack via a belt and ball-nut gear having a high transmission efficiency and higher torque assist, which can meet the needs of automobiles with higher demands for steering assistance. Figure 9 represents a generic EPSapa system with its main components. Table 2 represents different parameters of a standard EPSapa system.

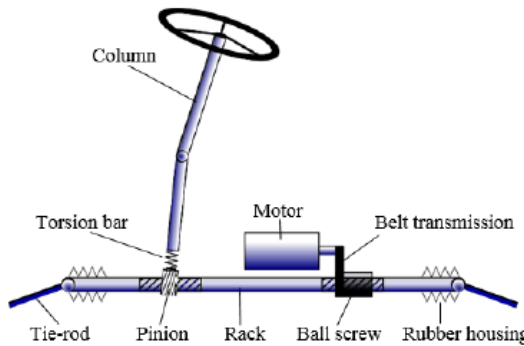


Figure 9: EPAS system with axle-parallel drive

#### EPAS Parameters

Table 2: EPAS Parameters

Parameters	Abbreviations	Value	Unit
Steering column inertia	$J_s$	0.03	$\text{kgm}^2$
EPAS motor inertia	$J_m$	$2.5 \cdot 10^{-4}$	$\text{kgm}^2$
rack mass + equivalent wheel mass	m	120.00	kg
steering column damping	$b_s$	0.20	Nms/rad
belt damping	$b_m$	0.005	Nms/rad
belt stiffness	$k_m$	40.00	Nm/rad
pinion stiffness	$k_s$	100.00	Nm/rad
pinion ratio	$r_p$	100.00	rad/m
ball-nut ratio	$r_g$	900.00	rad/m
belt ratio	G	3.00	rad/rad

The steering system was modeled as a 3-Dof system where, equations are divided into steering column equation, assist motor equation and rack equation.

**Steering column equation:**

$$J_s \cdot \ddot{\theta}_s = T_s - T_p \quad (1)$$

$$T_p = k_s \cdot (\theta_s - x_r \cdot r_p) + b_s \cdot (\dot{\theta}_s - \dot{x}_r \cdot r_p) \quad (2)$$

In Equation 1,  $T_s$  indicates driver applied torque on the steering wheel,  $T_p$  is the pinion torque and  $\theta_s$  is the steering wheel angle.

**Servo motor equation:**

$$J_m \cdot \ddot{\theta}_m = T_m - T_a \quad (3)$$

$$T_a = k_m \cdot (\theta_m - x_r \cdot r_g \cdot G) + b_m \cdot (\dot{\theta}_m - \dot{x}_r \cdot r_g \cdot G) \quad (4)$$

In Equation 3,  $T_m$  is the EPAS motor torque,  $T_a$  is the assist torque on the steering rack and  $\theta_m$  is the EPAS motor shaft angle.

**Rack equation:**

$$m \cdot \ddot{x}_r = T_p \cdot r_p + T_a \cdot r_g \cdot G - F_{tierod} \quad (5)$$

$F_{tierod}$  is the combined tierod forces from both wheels and, in case the steering model is tested in isolation from the vehicle model, as a basic assumption, tierod forces are calculated as a simple linear spring and a function of rack displacement with a stiffness  $K = 300000$  N/m. This value is derived from an estimation of the maximum lateral force which can be generated by the vehicle tires under a specific longitudinal velocity.

In order to understand the frequency response and behaviour of the EPAS system, a state space model of the EPAS was created. The outputs of a state-space can always be varied according to the quantities of interest.

$$\dot{x} = A \cdot x + B \cdot u \quad (6)$$

$$y = C \cdot x + D \cdot u \quad (7)$$

where,

$$x = [\theta_s \quad \dot{\theta}_s \quad x_r \quad \dot{x}_r \quad \theta_m \quad \dot{\theta}_m]^T$$

$$y = [\theta_s \quad x_r]^T$$

$$u = [T_s \quad T_m \quad F_{tierod}]^T$$

$$A = \begin{bmatrix} 0 & 1 & 0 & 0 & 0 & 0 \\ -\frac{k_s}{J_s} & \frac{-b_s}{J_s} & \frac{k_s \cdot r_p}{J_s} & \frac{b_s \cdot r_p}{J_s} & 0 & 0 \\ 0 & 0 & 0 & 1 & 0 & 0 \\ \frac{k_s \cdot r_p}{m} & \frac{b_s \cdot r_p}{m} & \frac{(-K_s \cdot r_p^2 - G^2 \cdot K_m \cdot r_g^2 - K)}{m} & \frac{-(b_m \cdot r_g^2 \cdot G^2 + b_s \cdot r_p^2)}{m} & \frac{G \cdot k_m \cdot r_g}{m} & \frac{b_m \cdot r_g \cdot G}{m} \\ 0 & 0 & 0 & 0 & 0 & 1 \\ 0 & 0 & \frac{k_n \cdot G \cdot r_g}{J_m} & \frac{b_m \cdot r_g \cdot G}{J_m} & \frac{k_m}{J_m} & \frac{-b_m}{J_m} \end{bmatrix}$$

$$B = \begin{bmatrix} 0 & 0 & 0 \\ \frac{1}{J_s} & 0 & 0 \\ 0 & 0 & 0 \\ 0 & 0 & -\frac{1}{Mr} \\ 0 & 0 & 0 \\ 0 & \frac{1}{J_m} & 0 \end{bmatrix}$$

$$C = \begin{bmatrix} 1 & 0 & 0 & 0 & 0 & 0 \\ 0 & 0 & 1 & 0 & 0 & 0 \end{bmatrix}$$

$$D = \begin{bmatrix} 0 & 0 & 0 \\ 0 & 0 & 0 \end{bmatrix}$$

### 3.2 Vehicle model

The vehicle was represented using a bicycle/single-track model. This model was chosen due to its simplicity and effectiveness in representing the vehicle's behaviour. Initially, roll was not considered and tires were assumed to have a linear behaviour. The parameters which were used are presented in Table 3 and belong to a Volvo sedan. Focusing on lateral force and moment in the vehicle reference frame, Equation 8 and Equation 9 were derived [8]. Equation 8 was normalized with respect to  $v_x$  in order to have it as a function of the vehicle states of interest:  $\beta$  and  $\dot{\psi}$ , vehicle side-slip angle and vehicle yaw rate respectively. Figure 10 represents the bicycle model with different parameters.

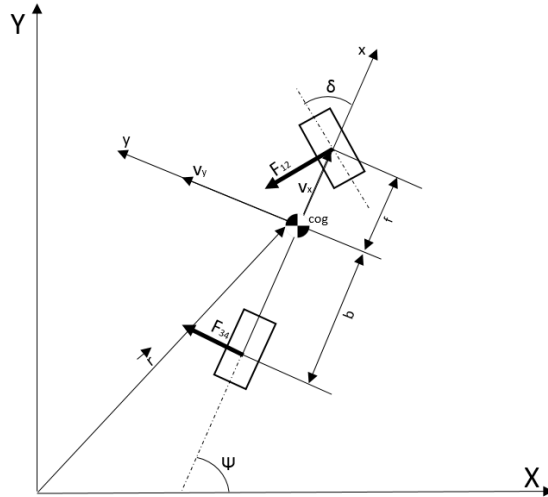


Figure 10: Bicycle model

Table 3: Vehicle Parameters

Parameters	Values	Units	Abbreviations
Front axle cornering stiffness	145000	N/rad	C <sub>12</sub>
Rear axle cornering stiffness	165000	N/rad	C <sub>34</sub>
Vehicle mass	1972	kg	m
Vehicle polar moment of inertia	3576	kgm <sup>2</sup>	J <sub>z</sub>
Distance from COG to front axle	1.24	m	f
Distance from COG to rear axle	1.69	m	b
Vehicle longitudinal velocity	—	m/s	v <sub>x</sub>

$$m(\dot{\beta} + \dot{\psi}) = -C_{34}\left(\frac{\beta}{v_x} - \frac{\dot{\psi}b}{v_x^2}\right) - C_{12}\left(\frac{\beta}{v_x} + \frac{\dot{\psi}f}{v_x^2} - \frac{\delta}{v_x}\right) \quad (8)$$

$$J_z \ddot{\psi} = -fC_{12}\left(\beta + \frac{\dot{\psi}f}{v_x} - \delta\right) + bC_{34}\left(\beta - \frac{\dot{\psi}b}{v_x}\right) \quad (9)$$

Having two linear differential equations and two vehicle states, a state-space of the vehicle model could be constructed. The selected output was chosen to be  $F_{tierod}$ , the lateral force developed by the front axle, assumed to be equal to half the tie-rod force for simplicity. This value is of interest because it is a direct input to the steering system. Therefore, in order to combine the state-space of the steering and vehicle models, determining the tie-rod force is required.

$$\begin{bmatrix} \dot{\beta} \\ \ddot{\psi} \end{bmatrix} = \begin{bmatrix} \frac{-C_{12}-C_{34}}{mv_x} & \frac{bC_{34}-fC_{12}}{mv_x^2} - 1 \\ \frac{bC_{34}-fC_{12}}{J_z} & \frac{-b^2C_{34}+f^2C_{12}}{J_z v_x} \end{bmatrix} \cdot \begin{bmatrix} \beta \\ \dot{\psi} \end{bmatrix} + \begin{bmatrix} \frac{C_{12}}{mv_x} \\ \frac{C_{12}f}{J_z} \end{bmatrix} \cdot \begin{bmatrix} \delta \end{bmatrix} \quad (10)$$

$$\begin{bmatrix} F_d \end{bmatrix} = \begin{bmatrix} -C_{12} & \frac{-C_{12}f}{v_x} \end{bmatrix} \cdot \begin{bmatrix} \beta \\ \dot{\psi} \end{bmatrix} + \begin{bmatrix} C_{12} \end{bmatrix} \cdot \begin{bmatrix} \delta \end{bmatrix} \quad (11)$$

### 3.3 Steering behaviour study

It is important to understand the dynamic behaviour of the basic analytical models before experimenting with a HiL environment due to its increased complexity which can alter the basic system behaviour. A study of the effect of adding an EPAS system in the loop was also conducted.

Due to the large quantity of parameters which characterize the steering and vehicle models, a parameter variation of each single variable was not performed: it was more interesting to study the system behaviour from a general perspective and the impact of the EPAS operation on the system dynamics. Thus, it was decided to run four different simulations:

- Standard, non-assisted, rack and pinion steering system.
- Standard, non-assisted, rack and pinion steering system with EPAS motor inertia added.
- Standard, assisted, rack and pinion steering system with EPAS boost curves.
- Standard, assisted, rack and pinion steering system with complete EPAS ECU logic.

These simulations, each with increasing system complexity, should provide an explanation of how added variables (motor inertia, ECU functionalities) affect system dynamics. Since the focus of this research is on steering systems with EPAS, most metrics used for the objective evaluation of steering performance relate to SWT, SWA and  $a_y$ . Therefore, the analysis focuses on the following transfer functions:  $SWA/SWT$  and  $a_y/SWT$ .

Figure 11 shows the Bode plots for the four different simulation runs. The first curve has roughly two peaks in both gain plots even if they are difficult to identify due to the scaling (it was decided not to normalize the plots in order to highlight the effect of the EPAS on the gain). These peaks belong to the natural frequencies of the vehicle and steering

systems.

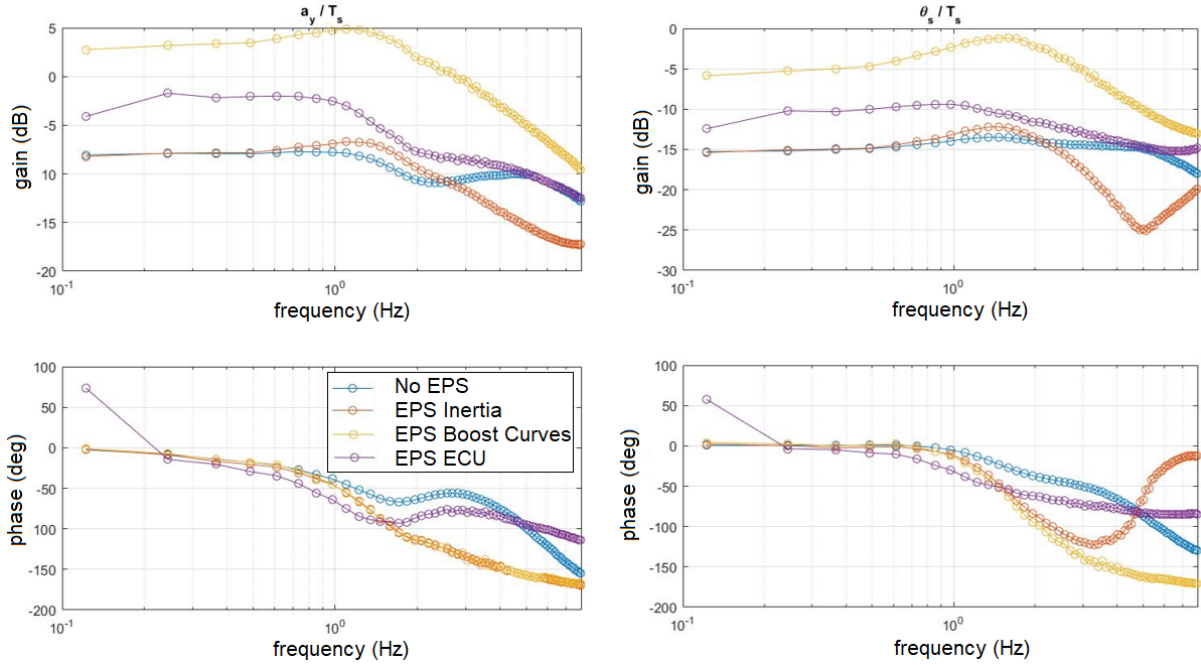


Figure 11: Frequency Response Analysis of Vehicle and Steering models.

1. The EPAS is not included in the model (blue).
2. The EPAS, belt and ballnut gear are modeled, but no assist is given (orange).
3. The EPAS is operational, but only uses its basic boost curves function (yellow).
4. The complete EPAS ECU is modeled, meaning the motor also uses functions such as inertia compensation, damping, steering return etc (purple).

If a non-operational EPAS is added to the steering system (second curve), one might counter-intuitively not expect to see a large difference compared to the original system, due to the negligible inertia of the EPAS. However, it must be kept in mind that in a EPASapa, which is the power steering system of interest in this thesis work, there is a relatively large ratio between the EPAS motor and steering rack that is introduced by the belt and ball-nut gear. This results in an increase of rack mass of three orders of magnitude due to the equivalent mass of the EPAS motor. As a consequence, the second curve shows a more pronounced peak and lower bandwidth in the gain plots. It must be underlined that, due to the use of a specific friction model, the peak is not as pronounced as expected. In the phase plots, the output/input delay increases quicker compared to the first curve due to the addition of this substantial equivalent mass.

If the EPAS boost curves functionality is activated, the combined system responds according to the third curve. There is an evident increase of gain even at low frequencies due to the motor assist, but the resonance peak, limited bandwidth and delay are still present due to the added equivalent mass.

Adding the full EPAS ECU model (fourth curve) substantially changes the frequency response of the combined system. On average, the gain is larger compared to the system with a disabled EPAS or with no EPAS at all, which is intuitive since the motor

always gives additional assist for a given driver torque, resulting in increased response values. However, compared to the third curve, the gain is lower, the resonance peak is smoothed/removed and the system response is less sensitive to the frequency of the input. This behaviour is caused by the additional features which the ECU provides. Examples are inertia compensation, damping and steering return. Analysing the phase plots, at low frequencies the fully modeled EPAS has a slightly higher delay, but above 1.3 Hz the opposite is true.

Overall, it is clear from the frequency response analysis that a realistic EPAS does much more than simply assisting the driver. All of its functions significantly affect the dynamic behaviour of the combined system.

## 4 Verification Method

Since the goal of the project was to determine the performance of the HiL steering rig, two additional models were developed using Matlab/Simulink and IPG Carmaker which represent the HiL system at different degrees of complexity. This section is aimed at explaining these models and their purpose.

The MiL was developed using Matlab/Simulink only and it is the simplest representation of the HiL. The EPAS operation is simulated by simple boost curves and the vehicle and steering models are self-developed or implemented (from already existing models). The SiL uses IPG Carmaker vehicle and steering models and the real EPAS ECU logic provided by the supplier. In both cases, the HiL system is modeled by two lumped masses, representing the servo and EPAS motors, and a spring-damper system in between the two representing the torque sensor. Finally, the real HiL setup is also briefly explained.

For this thesis work, Figure 12 shows in simple terms the relationship between the simulation type, its complexity and the design freedom involved with it. Due to its simplistic nature, the MiL is more suitable for quick tests and parameter studies, but results of low accuracy are to be expected. The SiL allows for better representation of the final system and it was indeed used for realistic predictions of the HiL performance.

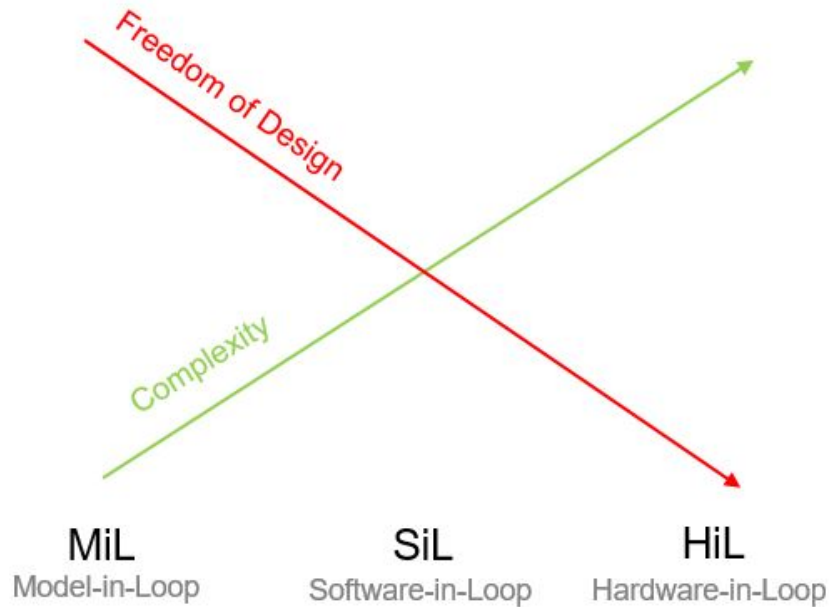


Figure 12: Characteristics of MiL, SiL and HiL

### 4.1 Model in Loop

#### 4.1.1 Model description

There were two reasons for using the MiL. Primarily, a general understanding of the simulation flow and steering system modeling could be gained. Secondly, a rough but fast system performance analysis could be performed prior to working with the HiL.

The MiL is a simplified analytical model of the HiL rig. It consists of a steering model

(subsection 3.1) which does not include friction and a vehicle model (subsection 3.2) which is of lower complexity than the one used in the SiL. Moreover, it includes EPAS boost curves to emulate a coarse EPAS behaviour and a simplified model of the HiL environment, including coupled servo motor, torque sensor and EPAS motor. The boost curves take two inputs, driver torque and vehicle longitudinal velocity, and give the EPAS torque as output. The output is the EPAS torque. Figure 13 shows how the four different subsystems (steering model, vehicle model, HiL model and EPAS boost curves) are coupled to form a closed-loop system.

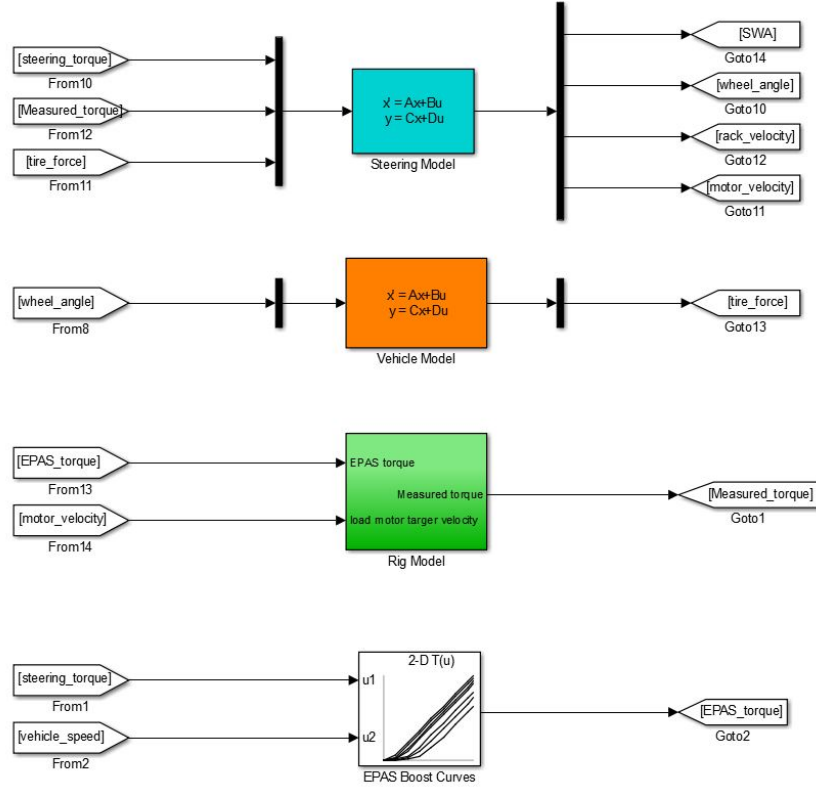


Figure 13: MiL Block Diagram

#### 4.1.2 Performance analysis

A secondary objective of the MiL use was to gather information on the HiL performance. A rough study on the effect of parameter changes on its performance was conducted. Due to the relatively low fidelity of the HiL, EPAS and vehicle model representations in the MiL, the focus was only on understanding the effect of HiL inertia changes and added transport delays. These quantities are the only two HiL model parameters which are introduced in the MiL.

First, a step position request was given to the servo motor. There are specific reasons why position request was selected and this is treated in more detail in subsection 5.4. This request was sent for two different servo drive PID settings and three different servo motor inertias, for a total of six simulations. Varying the PID tuning was performed to check if the control strategy had an impact on the effect of the inertia increase in the system on performance (bandwidth). As shown in Figure 14 and Figure 15, for both PID settings, increasing the inertia (at constant steps) results in a decrease of system bandwidth, which

is expected. It is important to underline that the term "system" refers to both the modeled LM position control loop and modeled LM hardware. This can be seen from the increase of response and settling time. This effect occurs because increased inertia acts as a lower cut-off frequency setting in a low-pass filter: the system filters out higher-frequency input content, but its gain drops at a certain frequency and the response gets phase shifted. Since this is valid for both PID settings, the trend of decreasing bandwidth for increasing inertia can be assumed valid irrespective of the controller tuning.

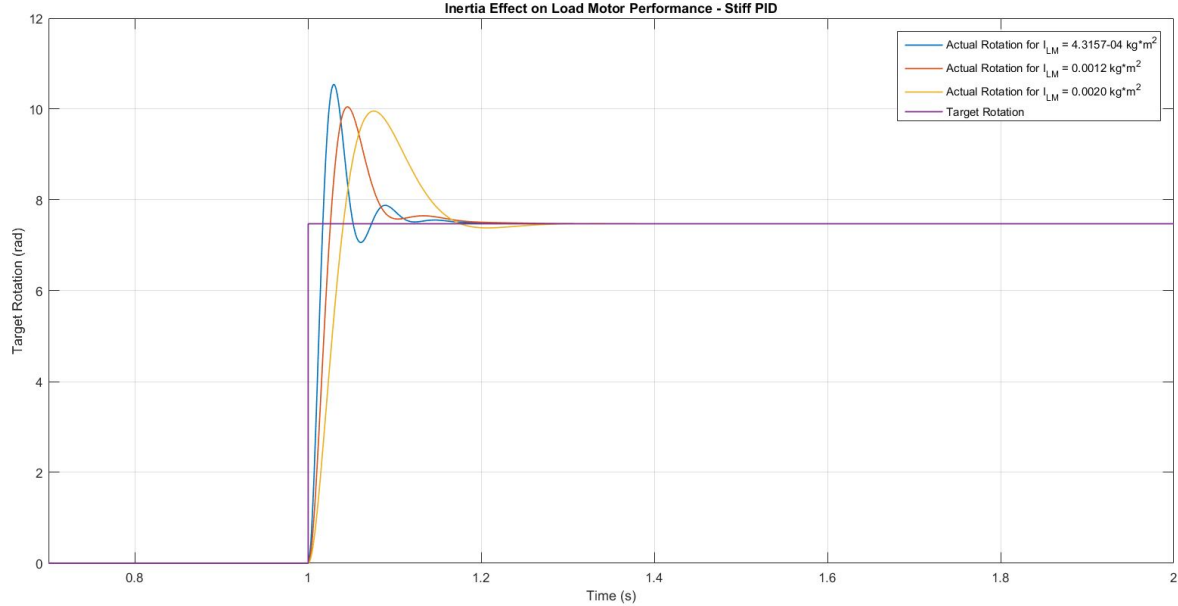


Figure 14: Inertia Effect on Load Motor - Stiff PID

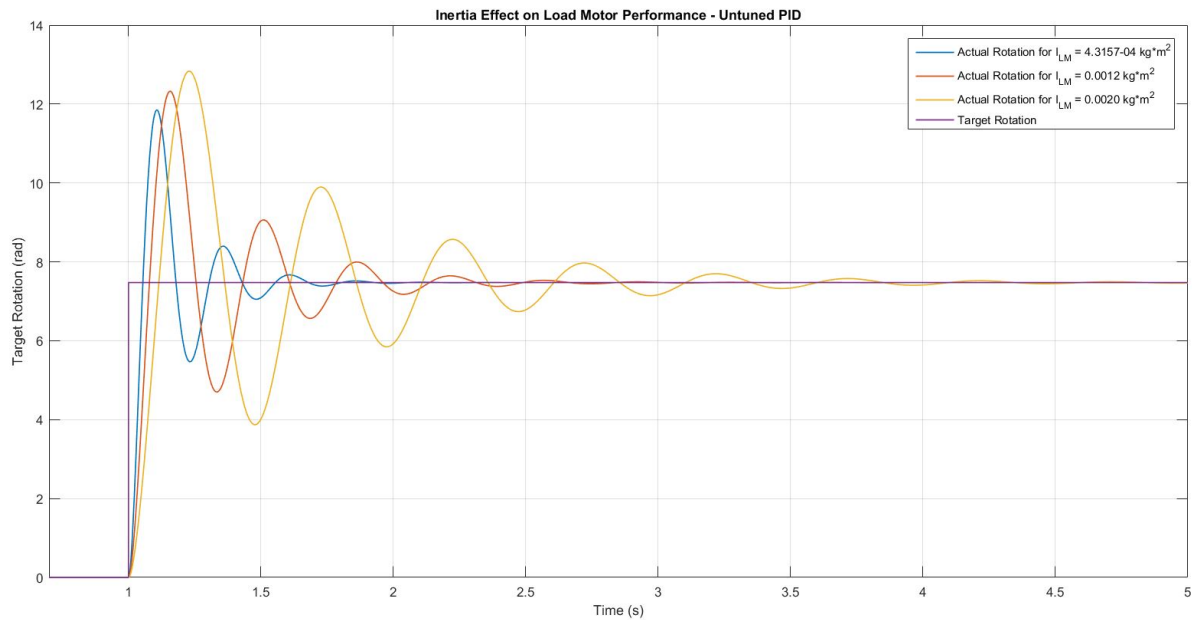


Figure 15: Inertia Effect on Load Motor - Untuned PID

Next, if a minimum time delay is introduced, the system becomes unstable (not shown in the plot). This is mainly due to factors present in the model which already introduce

delays in the torque sensor measurement, such as HiL inertia and torque sensor spring-damper model. This is an indication that, in the real HiL, even minor delays might render the simulation unstable.

## 4.2 Software in Loop

The SiL is a more complex version of the MiL. The reason for its use is to have a higher fidelity model of the real HiL compared to the MiL. In fact, in the SiL, IPG Carmaker steering and vehicle models are used and the real EPAS ECU logic provided by the supplier is used, just like in the real HiL system.

IPG Carmaker replaces the steering and vehicle models in Figure 13, while the EPAS ECU logic replaces the boost curves.

### 4.2.1 PSCM Software-in-Loop model

For proper comparison with the steering HiL rig, it is very important to have a simulation model containing IPG Carmaker and PSCM which are used in the HiL rig as discussed later. From the EPAS motor supplier, Volvo received an equivalent Simulink-based model of the PSCM which was flashed on the actual car.

As it can be seen in Figure 16, the model contains primarily three subsystem blocks which require specific inputs as defined by the supplier. The EPAS powerpack subsystem generates the assist torque which is fed back to the Carmaker vehicle model. The major inputs to the PSCM are torsion bar torque, vehicle speed, steering wheel angle and steering wheel angular velocity both for the SiL model and for the physical PSCM.

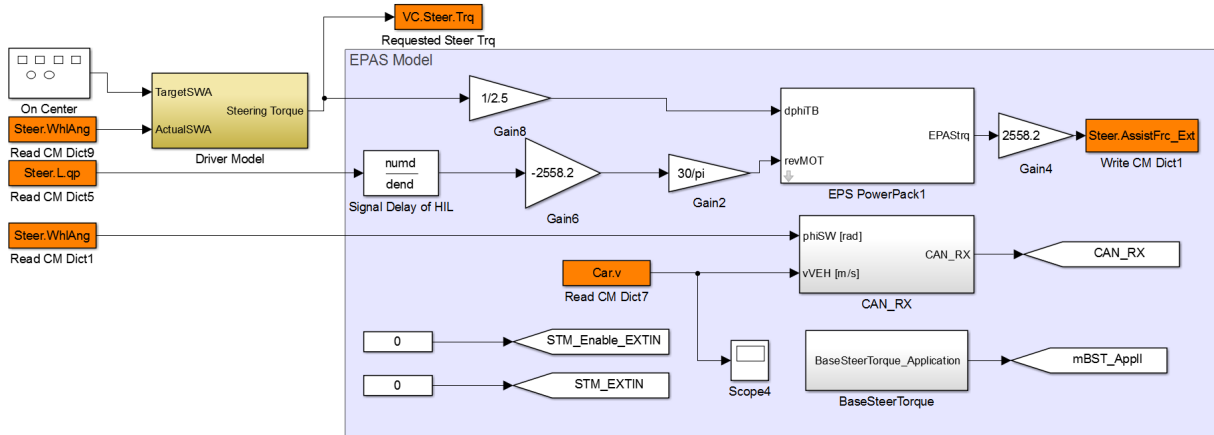


Figure 16: PSCM SiL model

### 4.2.2 IPG Carmaker implementation

Carmaker supports different model interfaces and one of them is Simulink. Therefore Carmaker for Simulink was used to integrate the PSCM SiL model.

Figure 17 shows the car and trailer subsystem consisting of steering, kinematics, forces, kinetics and the trailer subsystems. In this project, modifications were done inside the steering subsystem for the PSCM SiL model integration.

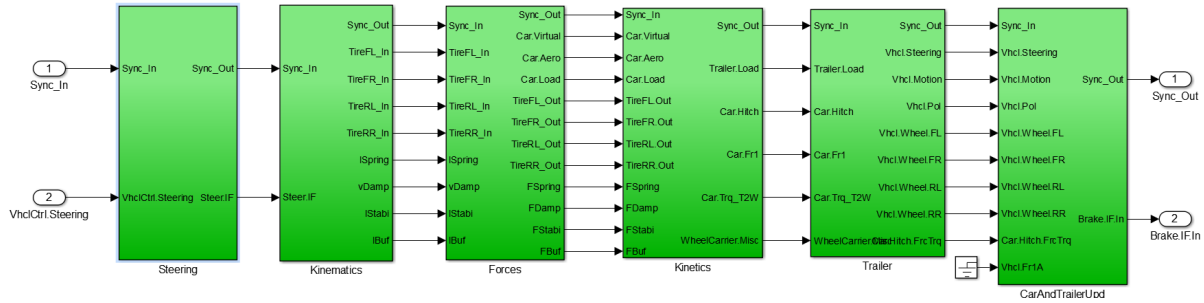


Figure 17: "Car and Trailer" subsystem of the Simulink Model in Carmaker

#### 4.2.3 Pfeffer steering model

Carmaker allows the use of three different kinds of steering models [9]. Table 4 refers to the different steering systems.

Table 4: Different steering systems

Model Name	Description
Static Steer Ratio	Angle model with 0 DOF
Dynamic Steer Ratio	Torque model with 1 DOF
Pfeffer with Power Steering	2 DOF model with EPAS

Pfeffer steering model in Carmaker consist of a mechanical module and an assisting module. In this project, only the mechanical module was used as the assist module was from the supplier.

#### Mechanical module

The mechanical module consists of the mechanical parts of the steering system such as steering wheel, steering column, rack and pinion etc. Figure 18 shows the structure of the steering system without the power assist module. This model allows steering wheel torque  $M_s$  or steering wheel angle  $\delta_s$  to be inputs "transferred" to the rack through the steering column, torsion bar and pinion. The steering column also includes column non-uniformity due to the double universal joints.  $S_R$  denotes the rack displacement and the assist from the EPSapa system is added as an assist force to the rack as  $F_{assist}$ .

During this master thesis, steering torque was used as the input in order to avoid Carmaker's untunable aggressive driver model. A simpler SWA error based driver model was implemented which will be explained later in the report.

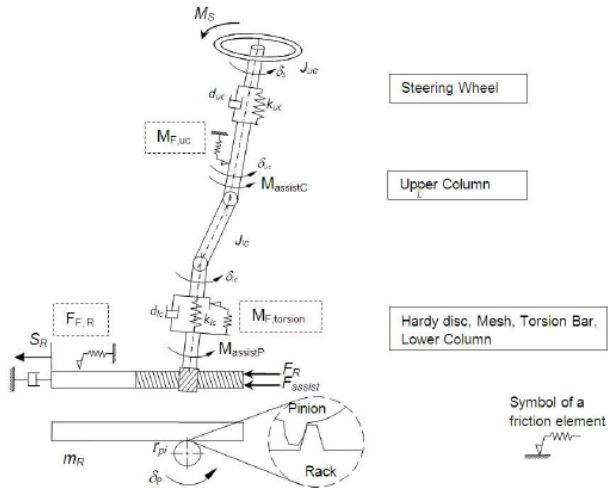


Figure 18: Mechanical module of the steering model with forces and direction of motion

#### 4.2.4 PSCM SiL model integration

The necessary inputs to the PSCM were used from Carmaker using *Read CM Dict* blocks of the Carmaker library in Simulink as shown in Figure 16. The PSCM in the real car has a speed encoder which measures the power steering motor shaft speed, but in the SiL model it is an input and calculated by converting the steering rack velocity to motor shaft velocity using gear ratio. Instead of torsion bar torque, steering wheel torque is taken as an input to the PSCM because, due to the parametrization of the Pfeffer steering model and partially due to the parametrization of the vehicle model, the torsion bar torque signal was noisy compared to the SWT. In any case steering wheel torque and torsion bar torque are almost same on a real car with minor delay due to compliance.

Output of the PSCM SiL module is the assist torque calculated according to its algorithm and sent back to the Carmaker model as an assist force calculated according to Equation 12 on the rack using *WriteCMDict* blocks.

$$F_{assist} = T_{assist} \cdot i_{ball-nut} \cdot i_{belt} \quad (12)$$

#### 4.2.5 PID based driver model

As defined earlier in subsection 2.5, most of the testing maneuvers are defined by steering wheel angle, but since steering wheel torque was used as an input to the steering model in Carmaker, a simple error feedback based driver model was implemented to convert reference steering wheel angle to equivalent steering torque to be used as an input to Carmaker. Figure 19 refers to the implemented driver model.

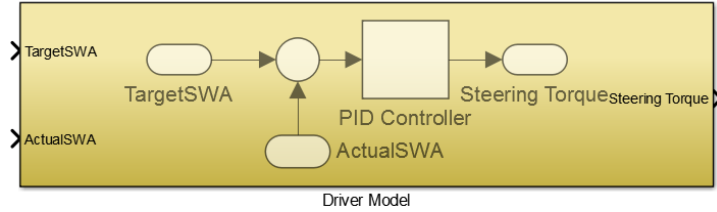


Figure 19: Driver model

#### 4.2.6 Delay modeling

Apart from comparing Carmaker vehicle simulation results and results from the HiL for different testing scenarios, one of the other most important use of the SiL model was to understand the effect of signal delays and added inertia in the HiL.

As discussed later in the section 5, from system identification a signal delay of 0.0525 s was identified between requested value and actual value for torque, position and velocity control of the load motor in the HiL rig. In terms of delay in the SiL model, the only input parameters of the PSCM that gets affected is the power steering motor velocity, so a signal delay was added in the motor velocity input channel as seen in Figure 16.

A pure time delay can be defined in two ways, using a "*transport delay*" in Simulink or with a pure transfer function of  $e^{-\tau \cdot s}$ , where  $\tau$  is the time delay. But  $e^{-\tau \cdot s}$  is not a rational transfer function so a second order Pade's Approximation for Dead Time is used [10]. As seen in Figure 20, there is a significant difference in phase response at higher frequency between delay using Pade's approximation and in pure delay.

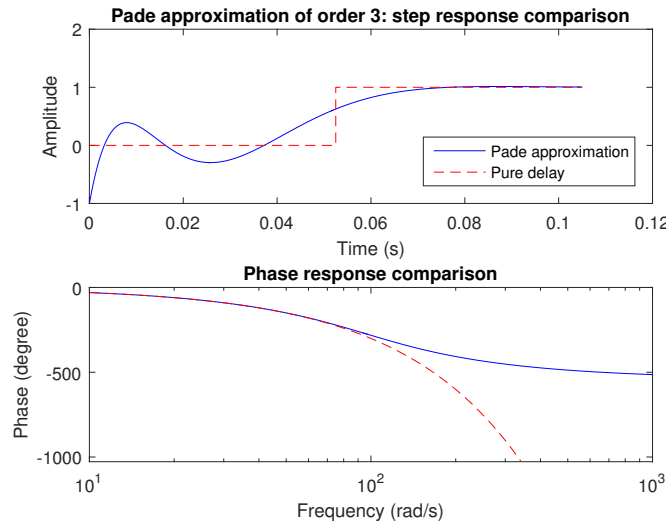


Figure 20: Pade approximation comparison for a step response

## 5 Powerpack HiL test rig

### 5.1 Literature review

As previously discussed to reduce cost and minimize development time for a new vehicle, hardware-in-loop simulation are becoming more and more popular. EPAS is a system mostly present in all the vehicle in production today.

Nowadays, most of the Original Equipment Manufacturers (OEM), including Volvo Cars are developing steering systems together with suppliers and sometimes insight into EPAS electronic control units (ECUs) is unavailable. Normally HiL testing involves testing vehicle components and its basic functionality but in this project the aim is to identify the performance of such a test rig in terms of complete electric power steering system development. PSCM includes a lot of complex functionality (e.g. active damping, active return, active safety maneuvers, etc.) and to avoid the PSCM going to error mode several different inputs (such as vehicle speed, steering wheel torque, etc.) are required that comes from vehicle simulation, more specifically from IPG Carmaker (HiL edition) in case of this project [11].

A conventional steering test bench often consists of several parasitic properties (e.g. inductance, capacitance and resistance) and as a result the EPAS motor and PSCM interact with a system which is comparatively different from the real car, which reduces the accuracy and quality of test results [12].



Figure 21: Example of conventional steering testrig

As in Figure 22, a comparatively simple powerpack steering test rig with less components is presented. Hardware combined with controls can result in a testrig with high bandwidth and a result quality which is difficult to achieve in a conventional test bench. In conventional test benches, the interface is at the connection of the rack where a linear actuator replicate the road disturbances as tie rod forces so the test rig can simulate these up to actuator bandwidth. On the other hand, using different load motor control strategies, even higher operation bandwidth can be achieved on a powerpack testrig. The biggest advantage of using a powerpack steering testrig is that it enables testing during the pre-development phase, even before a steering system physically exists. Concepts like steer-by-wire and designs like variable gear ratios can easily be tested: these can take a lot of time to be ready for a conventional test bench. Another advantage is the cost of a powerpack testrig is fractional compared to a conventional testrig and also compact.



Figure 22: Example of powerpack steering testrig

## 5.2 HiL architecture

The powerpack rig consists of a servo motor, an electric power steering motor, a torque sensor, a control cabinet with real-time PC and an user PC. Overview of the powerpack HiL consisting of different hardware and connections can be seen in Figure 24. Figure 23 shows the actual HiL at VCC.

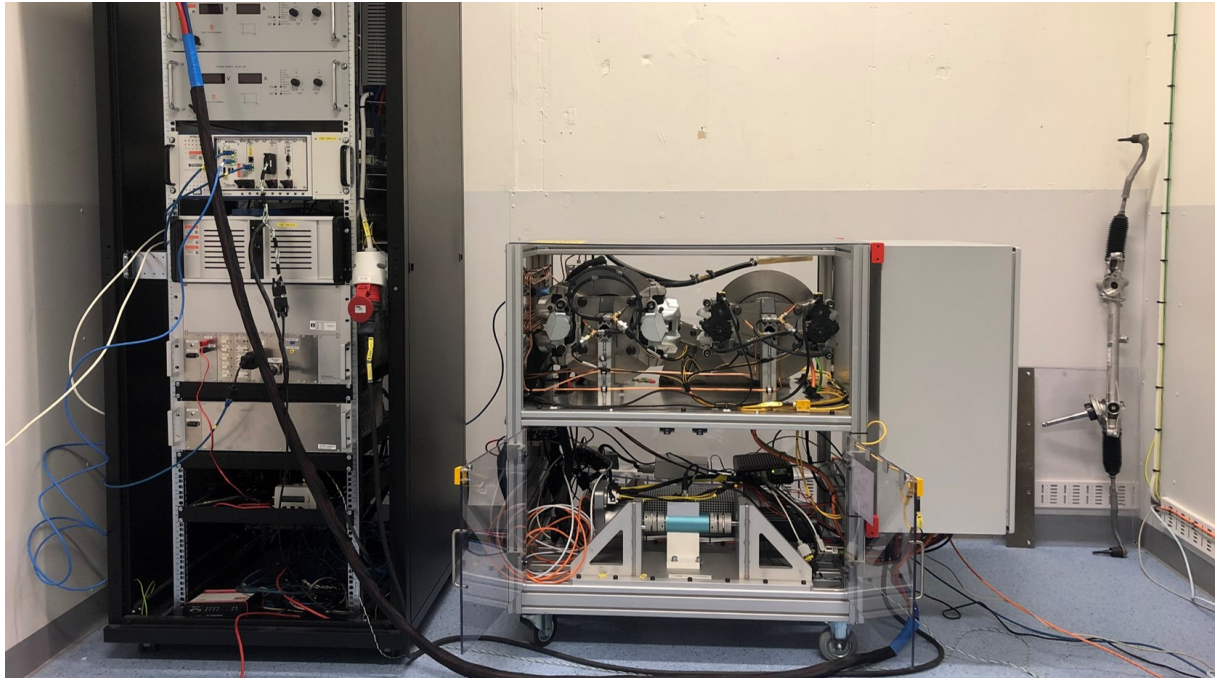


Figure 23: Actual image of the Powerpack HiL along with Brake HiL at VCC

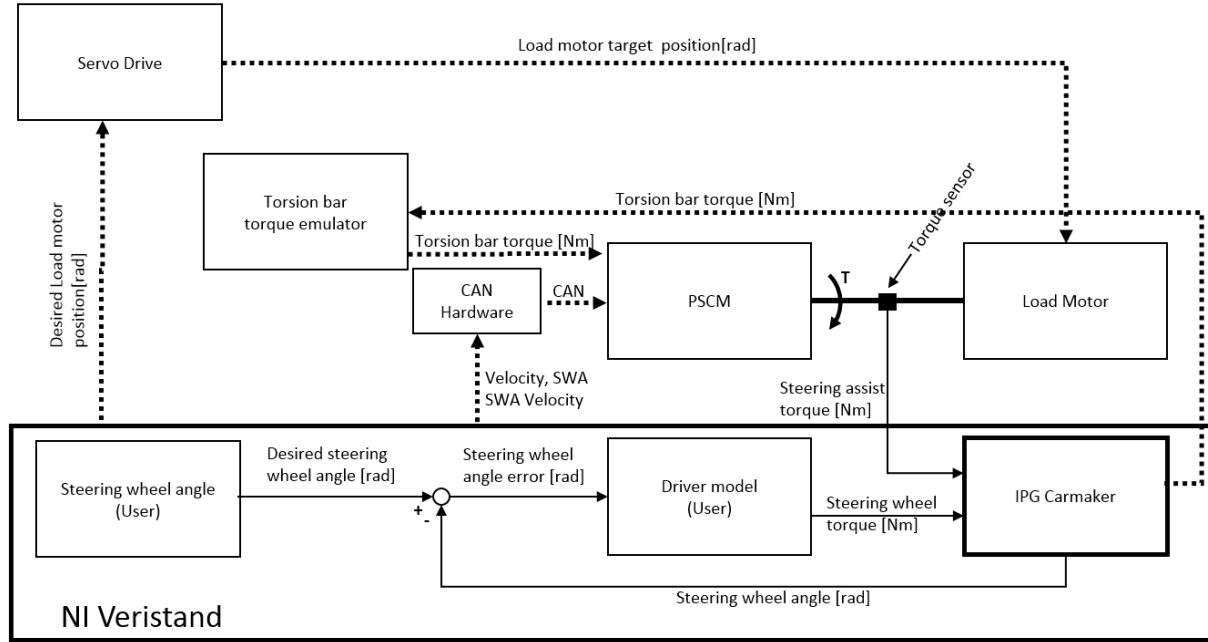


Figure 24: HiL architecture

As seen in Figure 25, the main part of the test rig consists of a load motor (4) which is connected using couplings (6) to the drive end of the torque sensor (7) and the measuring end of the torque sensor is connected using another coupling (5) with the EPAS motor (8). The EPAS consist of an ECU (PSCM) and servo motor which are the components present in a real car. As seen from Figure 24, the load motor receives a position request which is calculated inside IPG Carmaker and sent from NI Veristand to the servo drive which sends it to the load motor. The PSCM receives signals from Carmaker which come via CAN and a torsion bar torque emulator. The most important signal required by the PSCM to operate are torsion bar torque, vehicle velocity, steering wheel angle and steering wheel angular velocity.

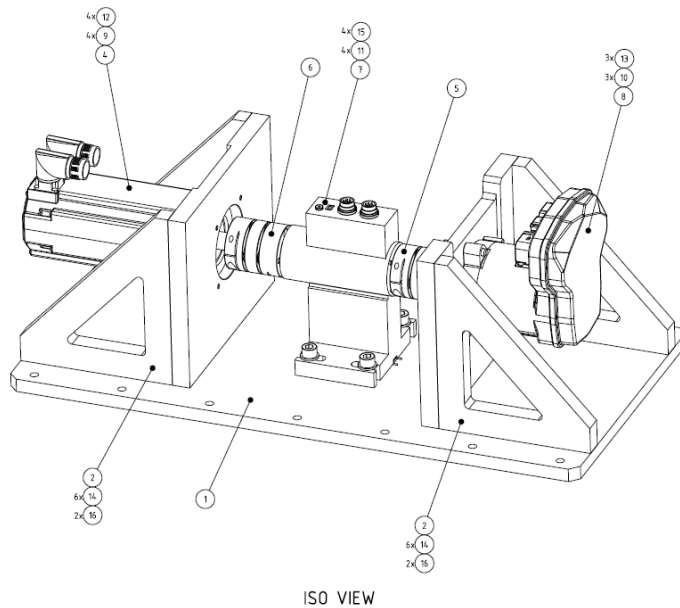


Figure 25: ISO view of the powerpack HiL

### 5.2.1 Hardware

The load motor is an AC synchronous servo motor from Kollmorgen, the torque sensor is a Kistler torque sensor, the real time environment is a National Instruments PXI system, the torsion bar torque emulator is a custom emulator box developed for specific purpose, the CAN hardware used for CAN simulation of the vehicle is a Vector VN8911 module.

### 5.2.2 Software

The control station is a normal PC is running NI Veristand, IPG Carmaker, Kollmorgen workbench and CANoe to communicate with the testrig. The operating system of the PC is Windows 10.

### 5.2.3 Communication

As seen in Figure 24, there are different communication channels running between different systems. The major two communication systems are EtherCAT which is an Ethernet based fieldbus system invented by Beckhoff Automation and CAN which is a standard communication protocol in a vehicle and was invented by Bosch. Communication between real-time system and servo drive for the load motor is EtherCAT and all the communication to and from the EPAS is using CAN [13].

## 5.3 System identification

System Identification [14] is a statistical method to build a mathematical model of a dynamic system where input and output data can be measured.

As the load motor is one of the most important components of the test rig, replicating conditions in a real car, a system identification was performed to understand its performance, i.e. open-loop bandwidth and measurement delay of the load motor I/O when connected with the complete test-rig.

There are many different ways to perform system identification. For the application of test-rig system identification, a *chirp signal* or a *swept sine signal* was used. The advantage of using a swept sine signal for this purpose was the fact that it was interesting to investigate frequencies up to 15 Hz and, in a swept sine signal, the frequency range can be specified easily using a limited amount of data [15].

The load motor used in the powerpack test rig has three different control loops. These are described below.

### Torque Control

Torque control is the most straightforward control strategy for servo systems. It involves the control of the load motor by feeding torque as an input to the system.

In its most basic form, the torque request can be calculated from an error minimization (using a specific control strategy, such as a PID controller) between the actual (measured) load motor applied torque and the target torque (requested). This strategy is shown in

Figure 26, where the full HiL model is shown. In this thesis work, the target torque would be coming as an input from the vehicle model.

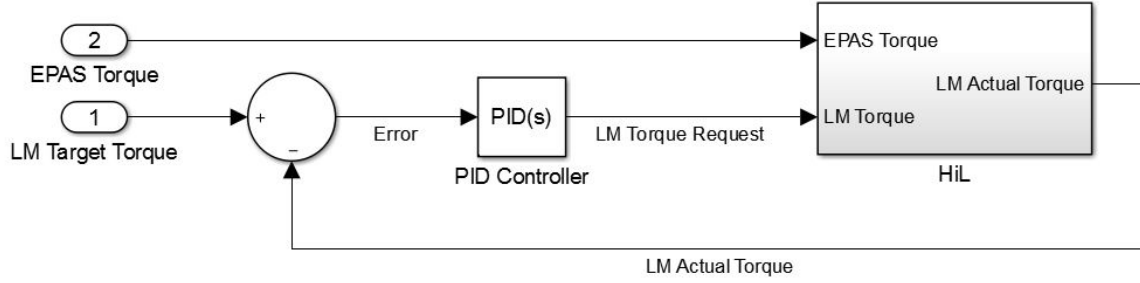


Figure 26: Generalized Load Motor Torque Control

Assuming a certain torque needs to be reached and maintained, the torque control loop is the one with highest bandwidth, but lowest accuracy compared to the velocity and position control loops [16].

### Velocity Control

Velocity control involves the control of the servo motor by feeding a target velocity as an input to the system. In its most basic form, the velocity request can be calculated in the same way as torque, using a specific control strategy such as a PID controller with an error input: between actual (measured) load motor velocity and target velocity (requested). However, in this case, torque control is still being performed, but in the form of a nested control loop within the velocity loop. This architecture is shown in Figure 27.

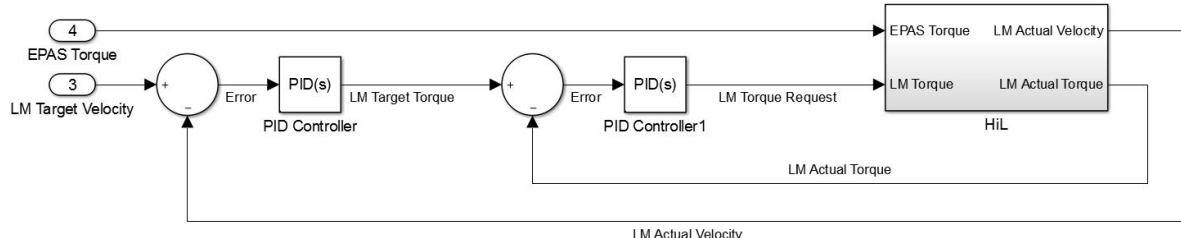


Figure 27: Generalized Load Motor Velocity Control

The velocity loop has lower bandwidth compared to the torque loop, however it provides higher position following accuracy.

### Position Control

Position control involves the control of the servo motor by feeding a target position as an input to the system. Once again, in the same way as the other control strategies, error minimization of the position is performed. In this case, the torque and velocity control loops are still implemented, but they are nested within the position loop. This architecture is shown in Figure 28.

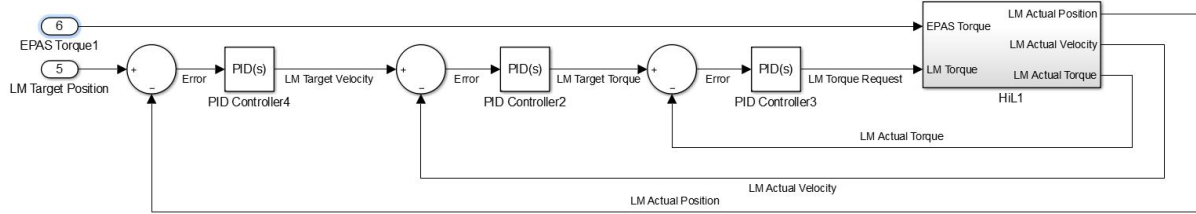


Figure 28: Generalized Load Motor Position Control

As expected, this is the control strategy which has the highest accuracy in terms of position. However, since it is the outermost loop, it is also the one with the lowest bandwidth of the three.

Now that the control strategies for the LM are clear to the reader, the discussion on the servo motor system identification can be continued.

The measurements were performed by sending a swept sine signal as an input to the load motor at the three different modes. The advantage of defining maneuvers in IPG Carmaker was used, as IPG Carmaker Real-Time was already connected to the load motor using Veristand. Output measurement was done using the encoder present on the load motor. Figure 29 represents a part of IPG Carmaker GUI used for generating swept sine signal.

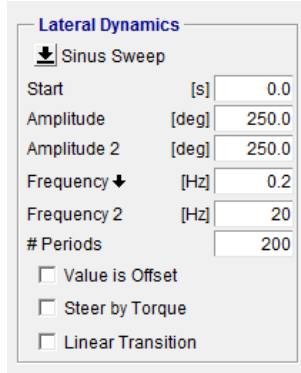


Figure 29: IPG Carmaker Maneuver GUI

The main objective of the system identification was to analyze the performance of the load motor, a transfer function and bode plots were generated, also the magnitude-squared coherence was estimated.

The reason behind analyzing the bode plot is the fact that it is a representation of the frequency response of the system and it is a combination of a gain plot (expressed in decibel or absolute scale) which expresses the magnitude of the transfer function i.e. ratio of output over input, and a phase plot (expressed in degrees) which expresses the phase shift between input and output. Coherence is the relation between the two signals or data sets. The magnitude of coherence lies between 0 and 1 and for an ideal linear system the coherence value will be 1. If coherence is less than 1 but greater than 0, then there is either noise in the measurement or the output is affected by other factors as well. Zero coherence means there is no relation between the two signals. For the purpose of system

identification, input and output signals of the load motor were used.

As it can be seen from Figure 30, the bode gain plot for all three types of control have a magnitude close to 1 between frequencies of 0.1 to 10 Hz, while position control performs comparatively better. It was expected to have an absolute magnitude of 1 which means the load motor can follow torque, velocity or position request accurately even with the shaft and the EPAS motor connected but not operational. Only for torque control, bode plot has a magnitude less than 1 at low frequency, the reason behind it is suspected to be the torque used to overcome the friction and it is dependent on the magnitude of torque as well, which means for low frequency maneuvers torque control will not be the perfect strategy to be used.

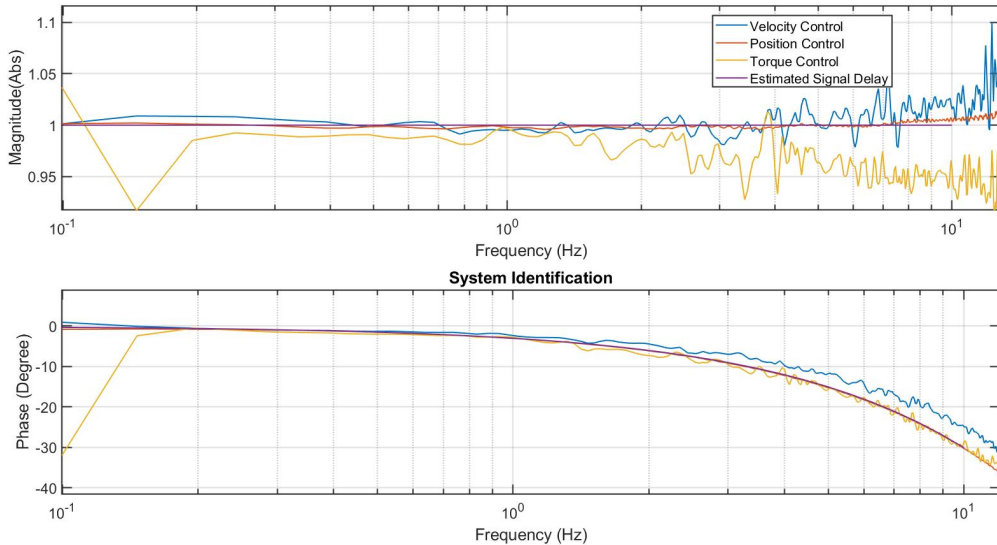


Figure 30: Bode plot of load motor system identification

In the bode-phase plot of Figure 30, all three control plots have similar nature and a negative phase change with increasing frequency represents a signal or measurement delay. Different techniques can be used to identify the delay, in this case a simple manual tuning method was used to match the phase plot of the identified system. A transfer function  $e^{-\tau \cdot s}$ , which represents a signal delay of  $\tau$  seconds, was plotted along with the identified transfer functions and by manual tuning the delay was found to be approximately 52.5 ms for torque and position control. Comparatively less delay was observed in velocity control as it can be seen from Figure 30. In Figure 31, all three controls exhibit quite high coherence over the frequency range up to 10 Hz, with position control performing comparatively better. Since frequencies less than 0.1 Hz is not of much concerned, coherence from very low frequency can be ignored.

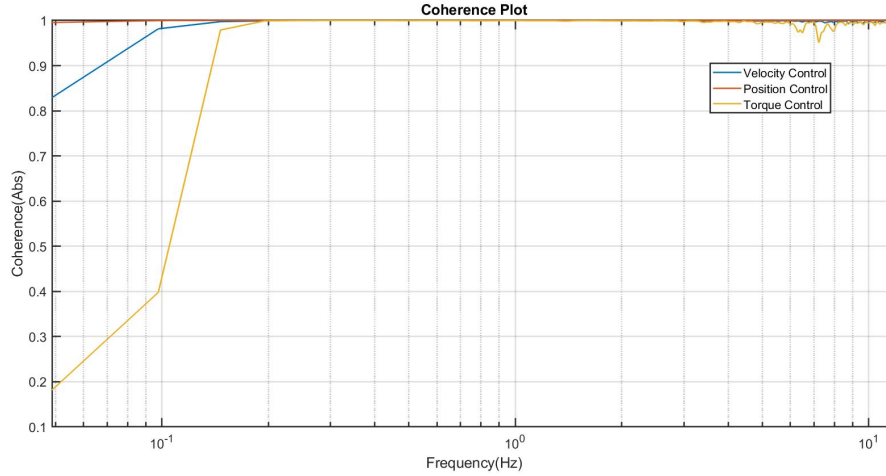


Figure 31: Coherence plot of load motor system identification

The static driving simulator, which will be explained in a later section, was also an important part of this project. Therefore, to further analyze if a similar signal delay exists in a servo motor of similar dimensions, a system identification was performed on the servo motor of the static driving simulator at Volvo Cars. This LM was from a different manufacturer. From Figure 32, the phase plot shows that a similar signal delay is present, which is identified as approximately 60 ms by manual tuning. The performance of the static simulator load motor was comparatively poor due to the presence of higher inertia components connected to it. Thus, for a servo motor having similar inertia and similar size, having a signal delay of 50-60 ms is normal.

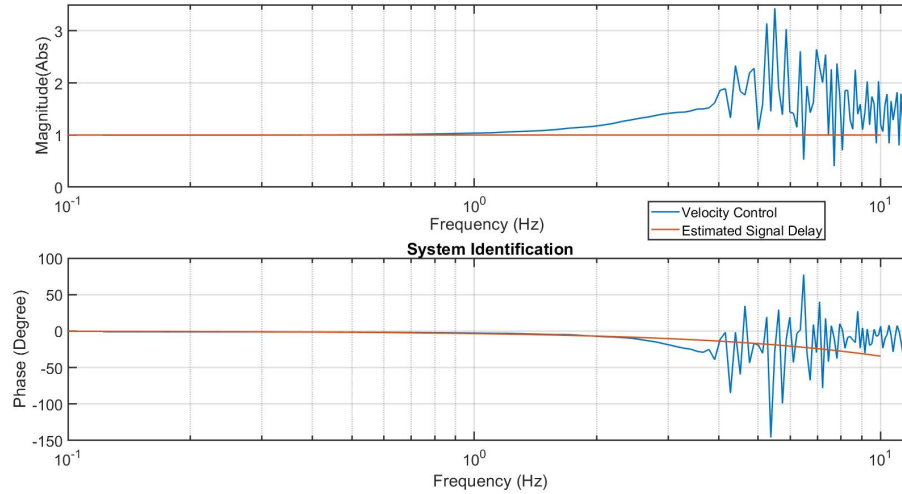


Figure 32: Bode plot from static simulator servo motor system identification

## 5.4 Steering test rig control

In the powerpack HiL, the load motor is used to emulate the dynamics of the EPAS motor shaft as on a real car. In Figure 33, the virtual cut refers to the position where the kistler sensor and load motor are connected, if compared to the test rig. The steering model running on real-rime system i.e. the Carmaker, consists of parts of the steering system

which are not physically present in the test rig (steering wheel, column inertia, rack mass, belt, ball-nut gear, torsion bar, pinion) and also the vehicle model which calculates the tierod forces.

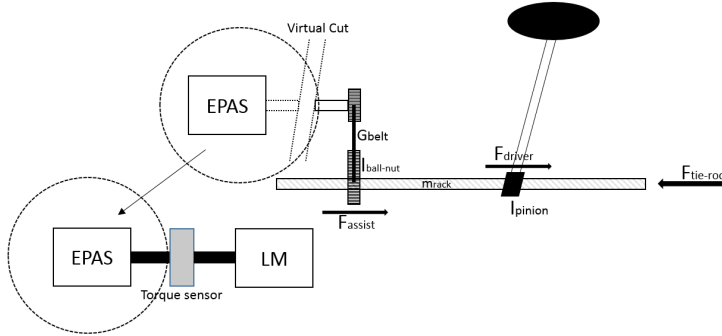


Figure 33: Steering system and powerpack testrig correlation

As shown in Figure 24, a position request is sent to the load motor. The position request represents the position of the EPAS motor shaft on the real vehicle. In the steering system, the rack is physically connected with the EPAS motor through a ball-nut gear and a stiff belt, assuming compliances to be negligible from rack to motor, position request for the load motor is calculated from the Carmaker steering rack position, which is one of the states of the steering model. According to subsection 3.1,

$$\text{Position request} = x_r \cdot r_g \cdot G$$

The measuring end of the kistler sensor is connected towards the EPAS motor, therefore it measures torque output of the EPAS motor. Since there are no physical components apart from the EPAS motor and PSCM, the measured torque from the EPAS motor which is equivalent to  $T_m$  in subsection 3.1 is converted to assist force on the rack and sent back as an input to the Carmaker steering model.

$$\text{Assist force} = T_{kistler} \cdot r_g \cdot G$$

According to the causality principle, a torque can also be requested to the load motor and position feedback to the steering model in Carmaker can be done, but due to practical limitations of Carmaker not allowing to overwrite states of the steering model, position control strategy was used for the load motor.

## 5.5 Autonomous driving mode test capability

Alongside advanced driver assistance system ADAS functionalities such as lane keeping assist and stability control, EPAS systems play a very important role due recent development of autonomous vehicles. Since in a level 5 autonomous vehicle there is no driver intervention or input, the vehicle is completely steered by the torque from the EPAS motor.

The PSCM receives a rack position request or a torsion bar torque request from the autonomous drive module in the vehicle. When it comes to testing Autonomous Driving

(AD) solutions, physical tests are normally performed after several verification steps using MiL, SiL and HiL models.

The powerpack steering testrig used in this project can be used for the purpose of testing AD mode steering. The EPAS powerpack used in this project was capable of AD mode driving so it was tested. The overall system architecture for AD mode testing remains same, the only difference is, that there is no steering wheel angle or torque input coming for the driver.

During this project, since the AD module was not available, rack position signal was sent to PSCM from a signal generator and the motion of the vehicle was observed in Carmaker. Since running AD mode was not the main focus of this master thesis project, further performance evaluation tests were not done, but the powerpack HiL rig has the capability to test AD Mode. Also, different redundancy testing and fault injection tests for the AD mode can be run on the HiL rig.

## 6 Static driving simulator

### 6.1 Overview

Driver-in-Loop DiL simulators have been increasingly employed in the automotive industry as an alternative to physical testing due to cost and time savings compared to prototyping and real-life testing. Driving simulators can be built with different goals in mind. Examples of areas of application for the driving simulator are vehicle dynamics studies, human behaviour analyses, driver training and ADAS functions development. Depending on the area of application, the driving simulator performance and complexity can vary [17]. For example, one way to categorize driving simulators can be the following: high-level, medium-level and low-level [18]. The higher the level, the more complex, costly and performance oriented the simulator is.

Steering system development is one of the most important fields where driving simulators are employed, mainly focusing on the subjective assessment of the steering system. As explained in subsection 2.5, OMs define steering system behaviour up to a certain extent but subjective assessment (SA) of the steering behaviour is extremely important since it represents what the driver will eventually feel while holding the steering wheel of the vehicle. Ideally, SA is done by expert drivers with real test vehicles but, in recent years, high-fidelity driving simulators can also be used for this purpose [19][20].

In this project, the aim was to include a powerpack HiL rig in loop with the driving simulator so that the physical EPAS motor along with the PSCM could be tested and its effect could be felt in first person by the driver. This allowed combining the main objective study of the HiL rig performance with a subjective analysis. The advantage of performing this study was given by the benefit of being able to validate the objective data with a subjective feel.

### 6.2 Architecture

The VCC static driving simulator is shown in Figure 34 and Figure 35. The cockpit is a re-adapted Volvo vehicle chassis and it includes all dashboard commands and displays, of which only the most important ones are operational. To get a more realistic feel of the vehicle while driving in the simulator, it is important to have correct seating, steering wheel position and field of view. The driver inputs come from the steering wheel, brake pedal, throttle pedal and, depending on the vehicle model in use, the shifter. The two pedals and the shifter have sensors which send the input values to the real-time PC which runs the vehicle simulation. The steering wheel is connected through a shaft to a torque sensor, friction bearing and a servo motor capable of providing feedback torque to the driver.

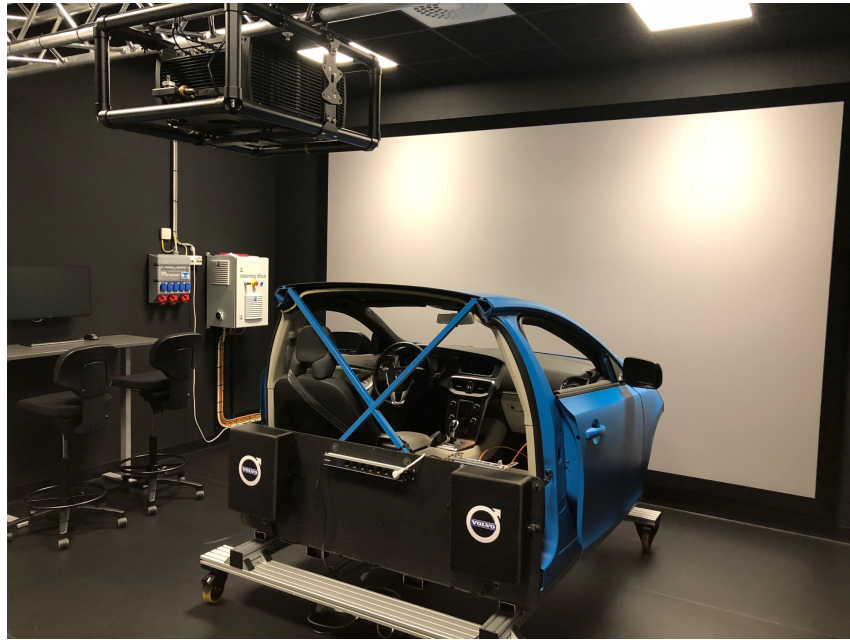


Figure 34: Static driving simulator at Volvo Cars Corporation

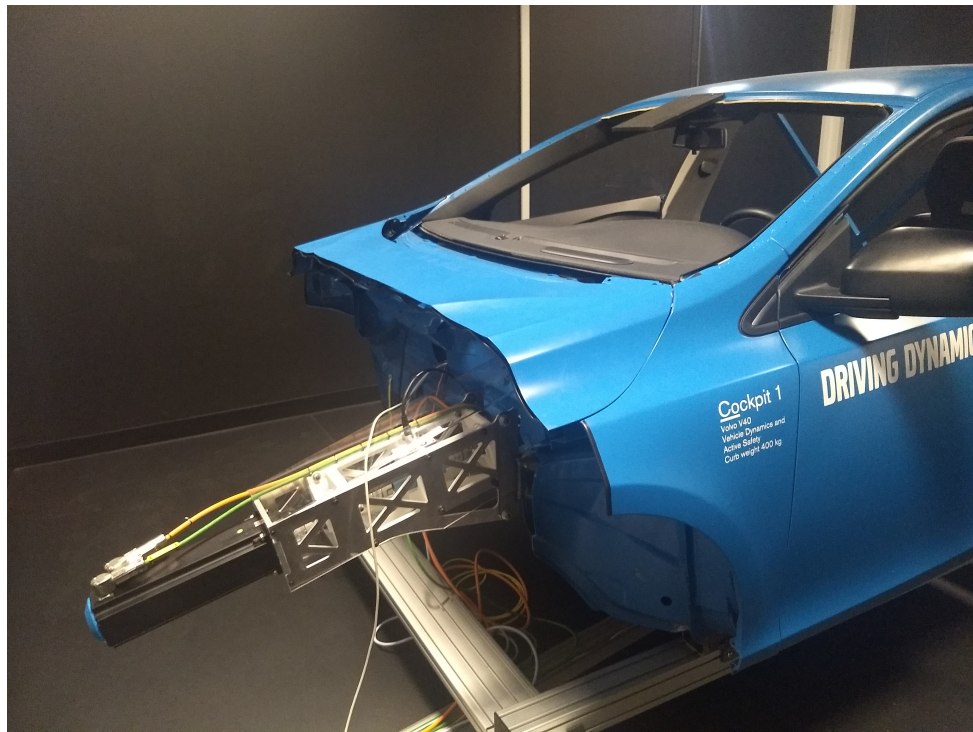


Figure 35: Static driving simulator at Volvo Cars Corporation - Steering Column

The static simulator can be run in loop with the vehicle model and for the purpose of this thesis both HiL and DiL were connected in loop with the real-time PC. In this way, the simulation complexity increases, but the results should also be increasingly accurate due to the implementation of an EPAS motor and PSCM in the loop. The architecture of choice for this project is shown in Figure 36.

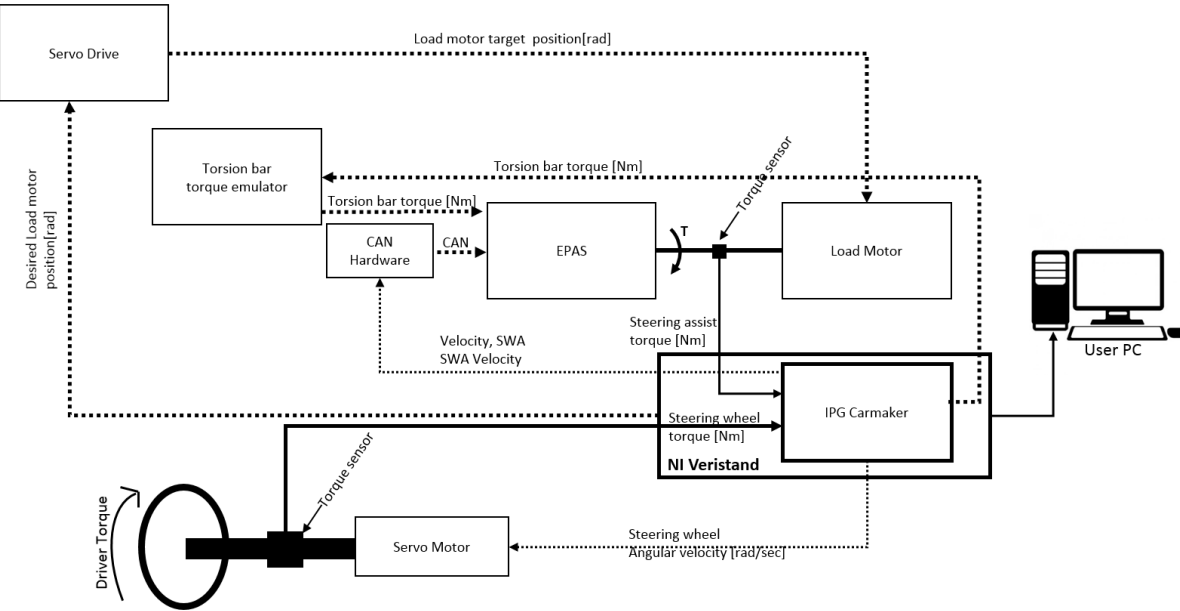


Figure 36: Driving simulator architecture with HiL

The torque sensor on the steering column is the same as the one used to compute the EPAS torque on the HiL system. However, the servo motor of the DiL is different compared to the one on the HiL. The two servo motors, being from two different manufacturers, have different control loops. Moreover, they were used with different control strategies (position control in HiL vs velocity control in DiL).

For running the driving simulator with the powerpack HiL rig, the HiL hardware was kept the same as explained in subsection 5.2. The additional DiL I/Os were added in the loop. As shown in Figure 36, instead of having a driver model responsible for the input to the Carmaker model, the real driver is responsible for the input, which is directly applied through the static simulator steering wheel. The torque sensor on the steering column measures the driver torque and sends it to the Carmaker model as input. The Carmaker model, based on the input from HiL, inputs from DiL and internal vehicle parameters, calculates the rack velocity and sends it as output to the servo motor coupled to the steering wheel. The main reason for sending a velocity request in the DiL is related to safety: sending a position request as in the HiL servo motor case results in unsafe motor jerks of greater severity compared to velocity control (in case of a situation of loss of system stability). Moreover, torque control is not used due to causality reasons: the Carmaker model already requires torque as an input due to the mechanical nature of the model. The throttle, brake and gear inputs are not shown in the diagram because of the nature of the vehicle model and manoeuvres: the vehicle is modeled with an automatic gearbox and manoeuvres of interest only involve constant longitudinal velocities.

## 7 Results

One of the main task in this thesis was to find out the performance of the powerpack HiL rig in terms of testing steering DNA related OMs and compare results to the SiL simulation and real vehicle test data. Thus, in this section, the results of the SiL, HiL and real tests are presented and compared. The analysis was tackled on a per-maneuver basis.

Another important task was to run simulations by varying different parameters and understand if expected results from the variations matched the results from the HiL. Since enough data for comparison with real vehicle for parameter variation was unavailable, it was decided to perform the parameter variation study with the DiL and analyse data based on subjective feedback.

### 7.1 Comparison of Objective Metrics

As discussed in subsection 2.5, different objective metrics were identified by performing different maneuvers, mainly OC, LSS and HSS. In this section, comparison of important objective metrics according to maneuvers will be discussed.

#### 7.1.1 On-center

As seen in Figure 37, OMs numerical values are close to each other but not exactly same. For torque gradient and friction feel, results from the HiL and the test vehicle matches quite well but the results from SiL is comparatively lower. In Figure 38, it can be seen that the slope at the on-center region for real vehicle and HiL results are close but plot from the SiL is comparatively flatter and the hysteresis at 0 g from the HiL is more comparable to real vehicle measurements. The major reason behind this difference is the fact that in the SiL model, since everything runs in simulation and there is no measurement or sensor noise, the effect of the EPAS assist changes because of no presence of any low-pass filter or observer. The measurement from the real vehicle was not post-processed because understanding the trends was important and the OMs numerical values were taken from Volvo's database.

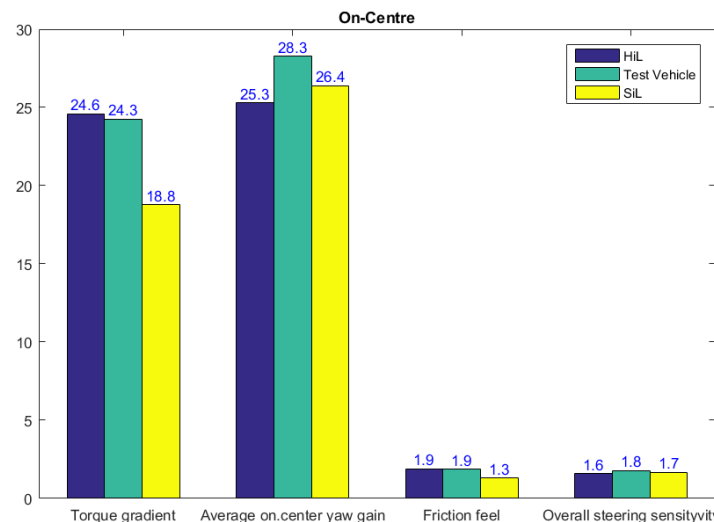
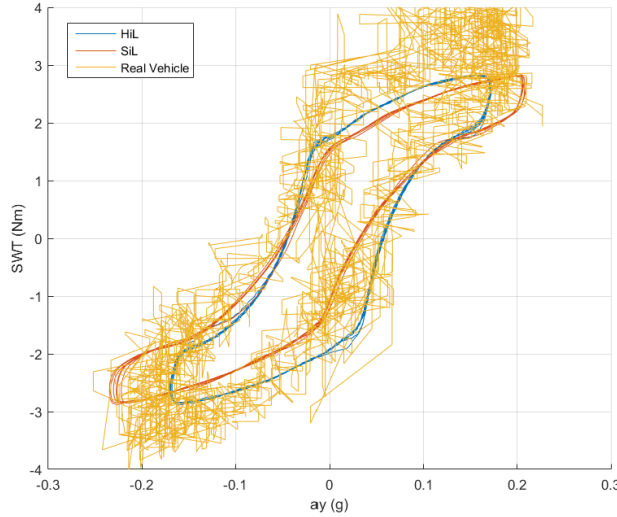
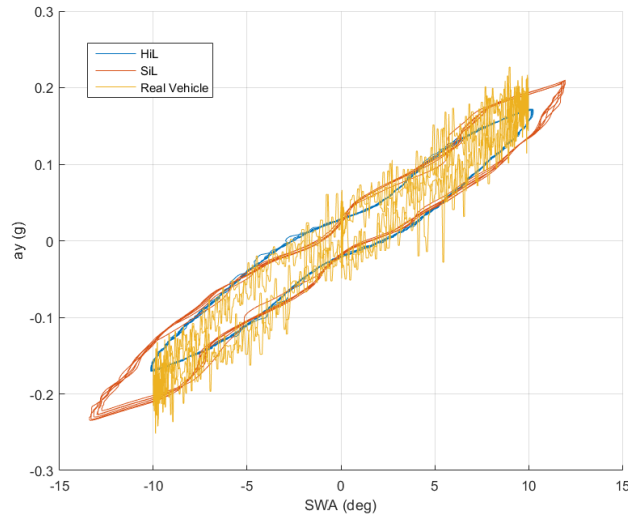


Figure 37: SDNA OMs for On-Centre maneuver

Figure 38:  $ay$  vs  $SWT$  for On-center

For average on-centre yaw gain, the resulting OM values from HiL and SiL are more comparable to each other, but for the real vehicle it is higher. Since vehicle yaw rate is a vehicle state, parameters of the vehicle model as well as inertia values affect the results. Due to the fact that vehicle model accurate validation was outside the scope of this project, these discrepancies are expected and the same analogy is valid for overall steering sensitivity because it is also derived from the states of vehicle and steering model. Figure 39 and Figure 40 represents the change of lateral acceleration with steering wheel angle and change of yaw rate with steering wheel angle respectively obtained from the on-center maneuver.

Figure 39:  $ay$  vs  $SWA$  for On-center

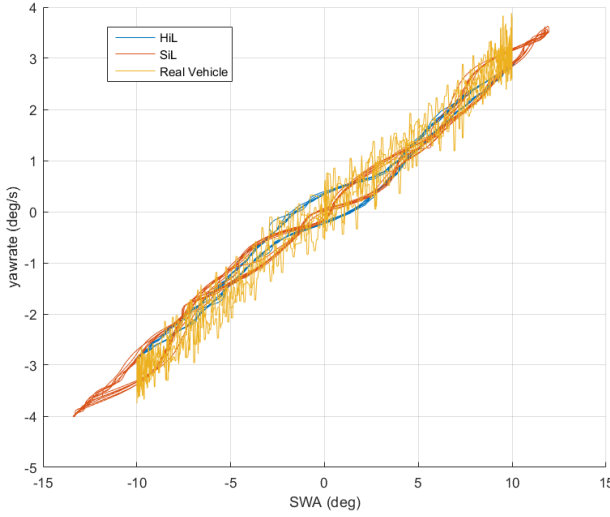


Figure 40: yawrate vs SWA for On-center

OMs derived from the SWA vs SWT plot, which is known as the hysteresis plot, are some of the most important to study for on-centre maneuvers. As seen from Figure 41, although OMs such as SWA at 0 Nm SWT and SWT at 0 deg SWA are comparable for HiL and real vehicle results, they are not close for SiL results. There are mainly two reasons for this discrepancy: the effect of low-pass filters as previously explained and the less aggressive driver model. OC is a maneuver as explained in subsection 2.5, where accurate steering wheel tracking is important to create proper sinusoidal steering input of 0.2 Hz, but in case of HiL and SiL simulation for this project, a simple PID based driver model was used as explained before, which was less aggressive in terms of reference tracking to reduce SWT fluctuation. In the real test vehicle, SWA tracking is done using a steering robot, which results in accurate results but fluctuating torque. Especially in HiL simulation, the robust and aggressive driver model could not be used because of the HiL sensitivity to noise and disturbances.

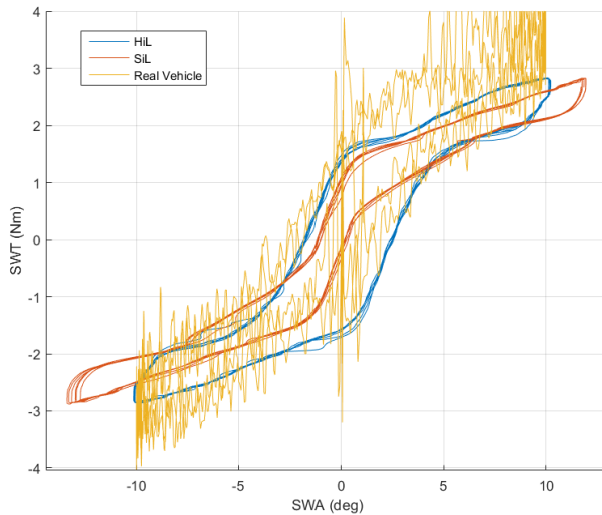


Figure 41: SWA vs SWT for On-center

As already discussed, one of the main reasons of discrepancy between the HiL and SiL models is the low-pass filter and it is quite evident especially in SWA vs SWT i.e. the hysteresis plot as seen in Figure 42. Since the kistler sensor measurement has a considerable noise, it can be eliminated with the use of a low-pass filter with very low cutoff freq (1-2 Hz), but since the overall transfer function gain of the low-pass filter drops with frequency, it reduces the assist force. For the purpose of OMs comparison a 4 Hz lowpass filter was used because higher cutoff frequency resulted in instability of the HiL.

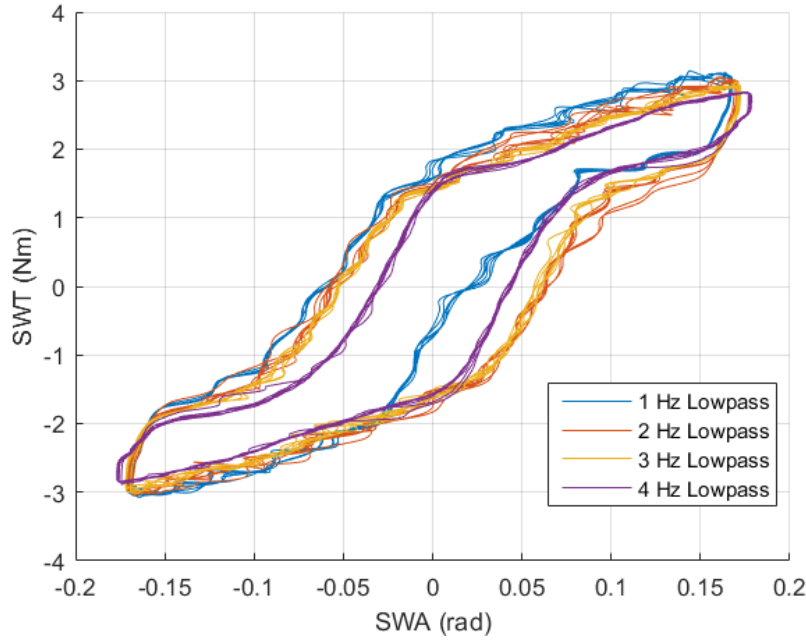


Figure 42: Effect of different low-pass filter cutoff frequency for kistler sensor measurement

### 7.1.2 Low-G swept steer

In Figure 43, the numerical values for the window and sensitivity ratio are very close but SWT at 0.05 G and torque deadband values are quite different. Since swept steer maneuvers are not really SWA based, the effect of a less aggressive and simpler driver model is felt less. Both SWT at 0.05 G and torque deadband considerably depend on friction and compliance of the real vehicle steering system, comparison with real vehicle measurement is not much useful, but since both SiL and HiL use the same steering model, reasons behind the discrepancy in OM values are of more interest. It is difficult to narrow down to a specific reason, but from an overall point of view, the discrepancy is most likely induced because of the delay in assist force generated due to the low-pass filter implemented to remove measurement noise from the Kistler sensor.

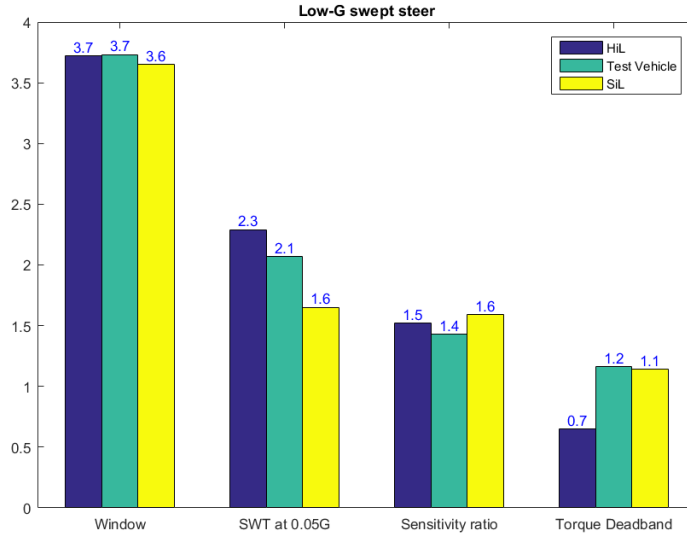


Figure 43: SDNA OMs for LSS maneuver

### 7.1.3 High-G swept steer

For HSS, as shown in Figure 44, major discrepancies can be seen for torque at 0.3 g or effort level and torque build-up cornering. Both of these OMs are related to comparatively higher lateral acceleration where tires are close to non-linear operating regions and tire models along with vehicle parameters play an important role. Torque build-up cornering is an off-center maneuver and although values from the real vehicle and SiL are identical, results from the HiL are lower. HSS is a maneuver performed at a speed of 80 km/h. At lower speeds, assist from EPAS is higher, so the effect of measurement noise from the Kistler sensor is amplified. Moreover, at lower speeds, in order to reach 0.3 g lateral acceleration, the required SWA is higher. Since a simple driver model was used, this induced oscillations when operating at higher SWA, resulting in a lower stability margin for the HiL rig which is the major reason of discrepancies.

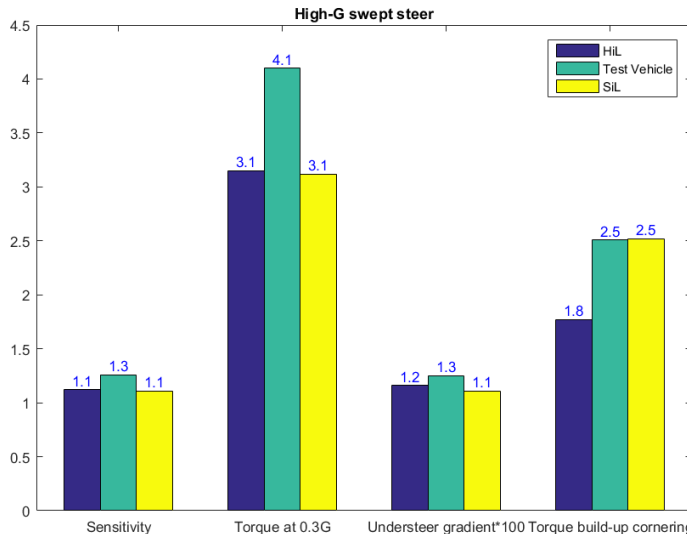


Figure 44: SDNA OMs for HSS maneuvers

## 7.2 Effect of parameter variation on Subjective Assessment

In terms of OMs, values are not exactly the same as obtained from the real vehicle testing, but they are very close except for a few specific OMs. Since vehicle model validation was not included in this project, the main interest was to investigate if the model is changed can it be perceived subjectively? A few of the significant ones which are discussed with possible explanations.

The steering system is one of the most important components of the vehicle in terms of vehicle stability, controllability and maneuverability. For steering system early-stage development subjective feedback is equally important when finalizing tuning of steering parameters, therefore subjective assessment of the steering behaviour was performed.

In order to evaluate subjectively, five semi-experienced drivers were asked to drive the vehicle using the static driving simulator as explained in section 6. The track was decided to be a slalom having 36 m gap in between cones and drivers were asked to maintain an average speed of 80 km/h throughout the maneuver. Apart from a fixed set of parameters for the steering system, it was also interesting to understand how much the changes in parameters or tires affected the steering system behaviour and if it was reflected on the static simulator as well.

The result from the parameter variation study can be seen in Figure 45. A single blinded study was performed, where in between every test-run with vehicle parameter changes, drivers were allowed to try the base vehicle for better subjective rating. To remove bias from the driver, changes were done at random and driver response was recorded. The effect of three parameter/model changes were studied. All drivers were asked to give feedback based on four different criteria:

- Response
- Controllability
- Torque cogging
- Torque gradient

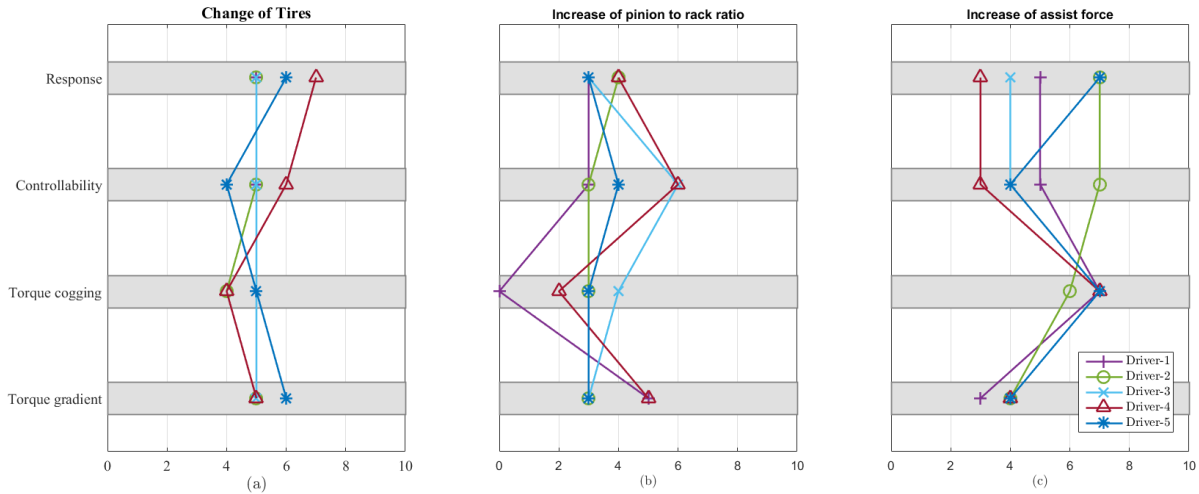


Figure 45: Effect of vehicle parameter changes on steering behaviour where (a) Effect of change of tires (b) Effect of change of pinion to rack ratio (c) Effect of increase in EPAS assist

These criteria are not standard for subjective assessment, but it was decided based on understandings crucial for this project. **Response** meant how well the car felt connected to the road, **Controllability** meant how well the driver thinks he could perform the maneuver without touching the cones, **Torque cogging** is the cogging on the steering wheel felt by the driver and **Torque gradient** referred to the severity of torque build-up when the car was steered in one direction. The base vehicle was given a prior rating of 5 for all four criteria as a reference to follow by all drivers.

From Figure 45, the change of tires did not result in significant change in subjective ratings for all four criteria, the main reason was, tire behavior was not significantly different, which resulted in no change of steering system behaviour and was expected.

Major change in subjective rating was observed when pinion to rack gear ratio was increased and the most affected criteria was Torque cogging, which was the main concern with DiL. Increasing the pinion to rack gear ratio resulted in less SWT requirement from the driver, which in turn results to less torsion bar torque i.e. less assist from the EPAS motor as decided by the boost curves. Since cogging on the steering wheel feedback originated from the HiL, as the magnitude of the Kistler sensor measurement gets lower, cogging on the steering wheel also becomes lower and similar behaviour was observed by all five drivers. Also, as a result the controllability of the vehicle increased due to better steering feel.

Torque cogging is the most concerning behaviour observed on the static simulator for DiL simulation as it is not felt while driving the real vehicle and the reason for its presence was identified to be the inclusion of the HiL, which is evident from the subjective assessment results. Subjective results from increased assist force on the steering rack further proves that the source of torque cogging is the HiL. Increased assist force results in amplifying the magnitude of the measured torque from Kistler sensor which induces more cogging.

## 8 Test rig control and limitations

In this section, the hardware and software limitations of the HiL rig are presented. Possible solutions are discussed.

### 8.1 Hardware limitations

In this subsection, the hardware limitations of the HiL rig are discussed. These can be found in all HiL environments.

#### 8.1.1 Added inertia

The HiL rig has additional components compared to a real steering system. A load motor, shaft, torque sensor and couplings add extra inertia to the system. Even if this inertia is relatively low (roughly  $5.93 \cdot 10^{-4}$  kgm<sup>2</sup>), the equivalent rack mass in the simulated steering model becomes substantial (going from 1.70 tonnes to over four tonnes). If this inertia is not compensated, the simulated steering system behaves differently compared to the real vehicle's steering system, which is unwanted. Moreover, it may cause stability issues due to the interaction with the EPAS model, where PSCM is tuned for a specific setup.

Two possible approaches were identified to solve this issue. From a hardware perspective, the servo motor could be mounted on a separate shaft and connected to the EPAS through a reduction gear (Figure 46). Using this method, the equivalent mass on the rack would theoretically be reduced.

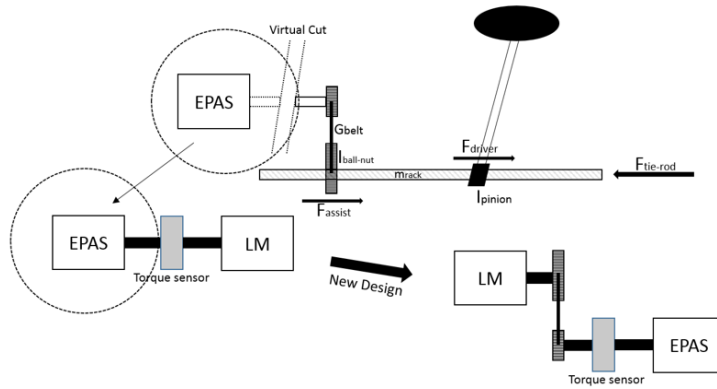


Figure 46: Suggested Hardware Change for Inertia Compensation

From a software perspective, the servo motor inertia compensation and control strategies should be studied more in depth in order to understand if the possibility to solve this issue using servo motor functions instead of changing the mechanical configuration exists.

#### 8.1.2 Torque ripple

When the servo motor was run in open-loop (EPAS inactive and no feedback signal to the Carmaker model), following a constant SW velocity input, the torque sensor measured a torque ripple of  $\pm 0.1$  Nm. As Figure 47 shows, the torque ripple has a constant peak

magnitude. This is due to motor design, more specifically the quantity and location of the motor windings [21]. The ripple is also present during closed-loop operation of the HiL and is a source of oscillations which may lead to instabilities.

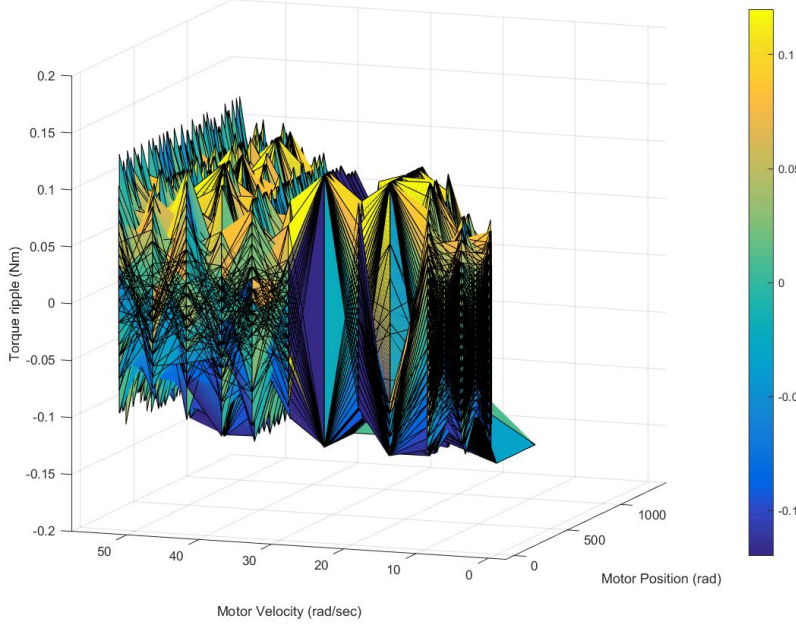


Figure 47: Servo Motor Torque Ripple

One possible solution which can eliminate torque ripple was identified. The servo motor has an embedded function which is purposely developed to remove torque ripple. More in-depth research must be done in order to implement this function correctly.

### 8.1.3 Transmission delays

Due to the nature of the HiL rig, transmission delays are introduced in the simulation. Hardware components such as electrical harnesses and circuits are some of the sources of signal delays, since it always takes a certain amount of time for a signal to travel from an output to an input port and it takes time for it to be processed.

The servo motor system delay was presented and discussed in subsection 5.3. In addition to this, there are many other system delays which could not be identified due to measuring limitations. The 50 ms servo delay combined with the other non-identified transmission delays can present a problem for the simulation. If the total delay goes beyond a certain threshold, the simulation may become unstable, due to the different systems (vehicle and HiL) not being synchronised.

Even if it is not feasible to eliminate all delays, it is possible to minimize a portion of them. One approach which was explored throughout this thesis work was the implementation of lead compensators. Lead compensators are transfer functions with one pole and one zero. Both zero and pole lay on the negative side of the real axis. The zero lays closer to the real zero value compared to the pole. This transfer function introduces phase lead into the system and increases the bode plot magnitude at higher frequencies. This increases

the closed-loop system robustness (increased stability margins), it allows tuning of the steady-state error and increases the system bandwidth. Equation 13 is an example lead compensator transfer function and Figure 48 is the associated bode plot.

$$TF = \frac{s + 1}{s + 2} \quad (13)$$

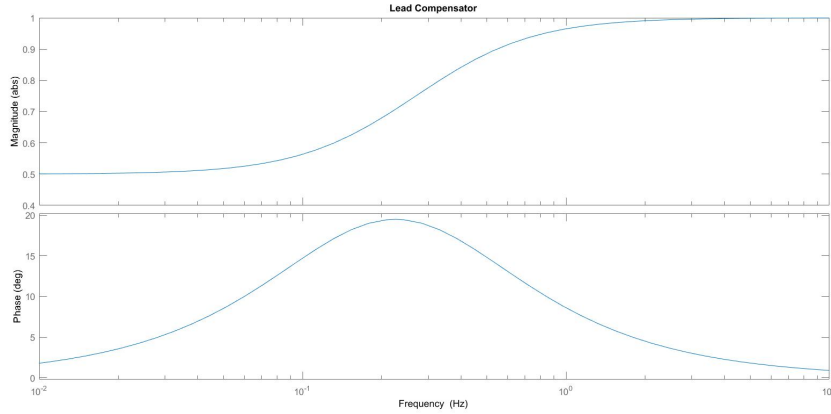


Figure 48: Lead Compensator Example

Therefore, it is suggested to try this approach in case additional substantial delays are identified in the HiL.

#### 8.1.4 Measurement errors

Measurement devices in the HiL rig should always be calibrated. The main sensor which requires calibration in the steering powerpack HiL rig is the torque sensor located between the EPAS and servo motor. Due to the closed-loop nature of the simulation, a calibration error will lead to wrong torque assist values being fed to the vehicle simulation and as a result, the rack motion will not be simulated correctly.

## 8.2 Software limitations

In this subsection, the software limitations of the HiL rig are discussed. These can be found in any HiL component which contains software of any kind, such as servo drives, torque sensors and real-time computer.

### 8.2.1 Servo motor control strategy

Due to the possibility of choosing between three servo motor control strategies, it becomes non-trivial to understand which is the ideal one to be used in a steering HiL rig. Thus, using an incorrect servo motor control can result in limiting the simulation fidelity or can even render it unstable.

After studying the EPAS software and testing the three different servo control strategies, the following conclusions could be drawn. First, it was understood that the EPAS motor has an embedded function which checks for the consistency between motor angle calculated using the input value to the PSCM and the motor shaft angle value. If there is an

error equal or higher than 10% between the two, the PSCM goes into a degraded mode, resulting in a non-functional EPAS. Second, in this specific project, it was not feasible to achieve a stable close-loop simulation while using torque or velocity control.

Based on the previous findings, it was opted for using position control of the servo motor in any steering HiL simulation and it is suggested to continue using this mode for future simulations.

### 8.2.2 Vehicle and steering models

The advantage of using a complex simulation model, assuming it is validated, is the access to higher fidelity results compared to simpler models. If this simulation model is not developed in-house, a third-party software is used: in the case of this thesis work, IPG Carmaker is the software which contains the full virtual vehicle model.

The disadvantage related to this case is the black-box nature of the computations occurring within the software. The solvers being used and the dynamic equation being formulated within Carmaker are not always accessible to the user. This means that any numerical instability and unwanted effects coming from the vehicle model are either not traceable or not solvable.

There are two straightforward approaches which can be followed to alleviate or solve this issue. A continuous communication with the IPG support could be maintained in order to understand all details of the vehicle simulation. Alternatively, an in-house steering model could be developed and used as an FMU (Functional Mock-up Unit).

### 8.2.3 Driver model

When running the HiL without the static simulator (no driver in the loop), the driver is simulated using a driver model described in subsubsection 4.2.5. Depending on the PID tuning parameters, the driver torque oscillations change. After testing, it was found that for good reference tracking (high stiffness driver model) the driver torque has high amplitude oscillations and the system may become unstable. For bad reference tracking (low stiffness driver model) the driver torque has low amplitude oscillations, but the SWA manoeuvre cannot be performed as described by the test standards.

The only solution is to change driver model. A neuromuscular driver model according to [22] was implemented only partially, but performance did not improve. If the HiL is used in isolation from the DiL, then additional driver models must be tested until one with relatively good reference tracking and minor torque oscillations is found. If the HiL and DiL are used together, then the issue is resolved since the driver model is substituted by a real driver.

## 9 Conclusions and Future work

This master thesis project was started with two main research questions with a primary focus being:

***Identification of EPAS HiL rig limitations in terms of steering system development using objective testing methods.***

In order to answer this question, an in-depth study using MiL and SiL simulations was performed before moving to EPAS HiL testing. Finalizing the control strategy for the HiL rig was challenging, but eventually position control of the load motor on the HiL was decided. Since the HiL simulation involves many closed loops between hardware and software components, closed-loop stability was difficult to achieve. Overall, HiL simulation stability was achieved by implementing solutions developed using MiL and SiL models, which mainly involved implementing different filters to reduce the effect of measurement noise.

As discussed in detail in section 7, a comparison study of SiL, HiL and real vehicle test results was performed. From the comparison, it was obvious that for some specific OMs resulting from three different scenarios are highly correlated and for those OMs EPAS HiL rig can be used. Less correlation between HiL simulation and real vehicle test results was found, mainly for OMs derived from maneuvers close to non-linear tire operation and OMs where model fidelity and validation plays an important role, e.g. friction and compliance in the HiL steering model was not perfectly validated with the real vehicle which resulted in less correlation of OMs.

Since most of the maneuvers required to define steering DNA OMs are SWA defined maneuvers and a simple PID-based driver model was used to avoid instability, OMs involving SWA were not comparable with real test results. Thus, for those maneuvers, it was more of interest to compare between the SiL and HiL results. Some minor discrepancies were found between OMs. There mainly derived from the presence of aggressive low-pass filters to remove measurement noise.

The second major part of the research question was the following:

***What can be changed in the future to achieve improved performance?***

From a general perspective, one of the greatest limitations of the HiL environment is the black-box nature of implemented analytical models, solvers and servo motor control. There are multiple approaches which can be followed to alleviate this issue. Developing in-house analytical models and co-simulation setups would make the vehicle model more transparent, but requires a substantial amount of development hours and would most likely not achieve the level of detail of the IPG Carmaker Virtual Vehicle Environment. Continuous communication with the servo motor suppliers is mandatory in order to understand the less intuitive functions of the servo drive.

From a specific point of view, the steering HiL rig performance can be boosted by splitting the focus between hardware and software. Hardware improvements should mainly

be focused to inertia and torque ripple/cogging compensations, transmission delays and systematic errors. While software improvements should be focused on the servo motor control strategy, vehicle and steering models, driver model and co-simulation techniques.

Lastly, but most likely the most important subject which requires a more in-depth study and further improvement, the coupling and interaction between the servo motor and EPAS motor resulted being one of the elements of concern for the HiL simulation. This is a very stiff coupling between two machines which are constantly applying torque to a common shaft, each using its own different control strategy. This can result in instabilities or oscillations of which the exact source is difficult to trace.

There can be two solutions to this issue. First, a reduction of the coupling stiffness could be introduced either from a mechanical or control perspective, which could reduce the oscillations but not fully solve the issue. Second, understanding the details of both servo motor and EPAS control logics could allow the user to perform control tuning for improving stability and overall performance.

## References

- [1] M.Harrer and P.Pfeffer, *Steering Handbook*. Springer.
- [2] Bosch, *New steering systems for tomorrow's mobility*, 2017. [Online; accessed 26-March-2019].
- [3] T. Hwang, "Development of hils systems for active brake control systems," in *SICE-ICASE International Joint Conference 2006*, IEEE, 2006.
- [4] N. Instruments, "What is hardware-in-the-loop?." <http://www.ni.com/sv-se/innovations/white-papers/17/what-is-hardware-in-the-loop-.html>, 2019. [Online; accessed 15-May-2019].
- [5] T. B. Bullock, "Servo basics for the layman."
- [6] www.ipg automotive.com, *Users Guide Version 7.1.1*.
- [7] K. D. Norman, "Objective evaluation of on-center handling performance, technical paper 840069," 1984. [Online; accessed 26-March-2019].
- [8] J. Jerrelind, "Lateral dynamics-the bicycle model," 2018. KTH Lecture slide.
- [9] www.ipg automotive.com, *Reference Manual Version 7.1.1*.
- [10] Mathworks, "pade." <https://se.mathworks.com/help/control/ref/pade.html>, 2019. [Online; accessed 06-May-2019].
- [11] M. Grunewald and M. Decker, "Functional testing of an electric power steering using hil simulations," in *5th International Munich Chassis Symposium 2014*, Springer Vieweg, 2014.
- [12] H. Briese, "Realistic dynamical testing of eps motors and ecus by means of a hardware-in-the-loop test bench," in *6th International Munich Chassis Symposium 2015*, Springer Vieweg, 2015.
- [13] EtherCAT, "Ethercat - the ethernet fieldbus." <https://www.ethercat.org/en/technology.html>. [Online; accessed 27-May-2019].
- [14] Wikipedia, "System identification." [https://en.wikipedia.org/wiki/System\\_identification](https://en.wikipedia.org/wiki/System_identification), 2019. [Online; accessed 25-March-2019].
- [15] Mathworks, "A practical application of new features of the system identification toolbox." <https://se.mathworks.com/company/newsletters/articles>, 2019. [Online; accessed 26-March-2019].
- [16] "Motion control tips- why is the bandwidth of a servo control loop important?," April 2017. [Online; accessed 27-May-2019].
- [17] G. B. et al., "The general motors driving simulator, 1994, section 6: Journal of passenger cars," *SAE Transactions*, vol. 103.
- [18] Y. S. Chiew and M. Hussein, "Kinematic modeling of driving simulator motion platform," in *IEEE Conference on Innovative Technologies*.

- [19] D. Katzourakis, “Design issues for haptic steering force feedback on an automotive simulator,” in *2009 IEEE International Workshop on Haptic Audio visual Environments and Games*, IEEE, November 2009.
- [20] G. G. Gomez, “Towards efficient vehicle dynamics development from subjective assessments to objective metrics, from physical to virtual testing,” doctoral thesis, trita-ave 2017:12, KTH Royal Institute of Technology.
- [21] “Motion control tips-understanding the distinctions among torque ripple, cogging torque, and detent,” August 2013. [Online; accessed 15-May-2019].
- [22] A. J. Pick and D. J. Cole, “A mathematical model of driver steering control including neuromuscular dynamics,” *Journal of Dynamic Systems, Measurement, and Control*, vol. 130, 2008. Issue 3.

